2008

Characterization of actuator behaviors of ferrogels obtained from physical and chemical cross-linking methods

Geunhyung Park
Iowa State University

Characterization of actuator behaviors of ferrogels obtained from physical and chemical cross-linking methods

by

Geunhyung Park

A thesis submitted to the graduate faculty

in partial fulfillment of the requirements for the degree of

MASTER OF SCIENCE

Major: Mechanical Engineering

Program of Study Committee:

LeAnn E. Faidley, Major Professor

Pranav Shrotriya

Qingze Zou

Iowa State University

Ames, Iowa

2008

TABLE OF CONTENTS

LIST OF TABLES

LIST OF FIGURES

ACKNOWLEDGEMENTS

First and foremost, I would like to acknowledge my major professor, advisor, and mentor Dr. LeAnn E. Faidley for her continued support, encouragement, and patience throughout the duration of my graduate studies. Her leadership and intelligence helped make my overall research work a successful and worthwhile endeavor.

Secondly, I would like to thank my research partner, Elease J. McLaurin for her invaluable knowledge and assistance. Even though she is in undergraduate programs in Iowa State University, she showed a great performance as my research partner. Plus, I also would like to thank all of lab mates in *AMISS, Active Materials and Intelligent Structure and Systems Lab.*

I would also like to thank my program of study committee, Dr. Pranav Shrotriya and Dr. Qingze Zou for their critique and suggestions. I am sure that their comments would help my future work developed and firmed.

Of course, I would like to extend my gratitude to all of my family and friends. Especially, my parents would have been incredibly supportive and encouraging throughout my graduate work in Iowa State University. Without the support of all those mentioned, none of this would have been possible.

Above all, I thank GOD to prepare and guide for my royal summons. I believe that my graduate work was entirely supported by my shepherd, Jesus. Lastly, I would like to express my deep thanks to Youkyoung for her priceless support and comfort in Jesus.

ABSTRACT

Ferrogels are soft polymer materials containing a filler of magnetic particles that allow the material to be activated by magnetic fields. These materials have shown capabilities for large strains, fast response, ease of synthesis and biocompatibility and have potential applications including artificial muscles, controlled drug release systems, and hyperthermia cancer treatment. In this work, the actuator behavior for a selection of ferrogel compositions and synthesis methods are characterized including their free strain and loading behavior. Samples were synthesized using either chemical or physical methods using Sodium Tetra-borate ($Na_2B_4O_7 \cdot 10(H_2O)$) or freeze-thaw cycle, respectively. Compositions consisting of PVA of 4, 8, and 12 wt% and magnetic particles of 1, 5, and 10 wt% were made. These samples were then tested for free strain and strain under loads of up to 4 times their weight by exposing them of fields from between 0.2 and 0.25T. Results show that softer samples with the largest amount of iron achieve the largest strains. Thus, chemically crosslinked sample with 4 wt% PVA and 10 wt% iron achieved the largest strain of almost 40%. However, low modulus samples exhibit low loaded capabilities with a blocked load of 1.7g identified. The physically crosslinked samples which were stiffer achieved very good loading capabilities with only a 20% strain decrease when loaded up to 400% of their weight. This translated in to an energy density of 320 J/m^3 making these materials very promising for actuator applications.

Chapter 1. INTRODUCTION

1.1. Present Smart Materials.

In recent years, new varieties of smart materials have been developed and used in industry due to the materials unique properties. The most commonly accepted definition of smart materials is that they are able to sense and respond to their environmental stimuli with particular change such as temperature, pH, electric and magnetic fields. Among smart materials, piezoelectric transducers (PZT) are one of examples which have been applied for energy harvesting and actuators by transducing mechanical energy into electrical energy and vice versa as shown in Figure 1.

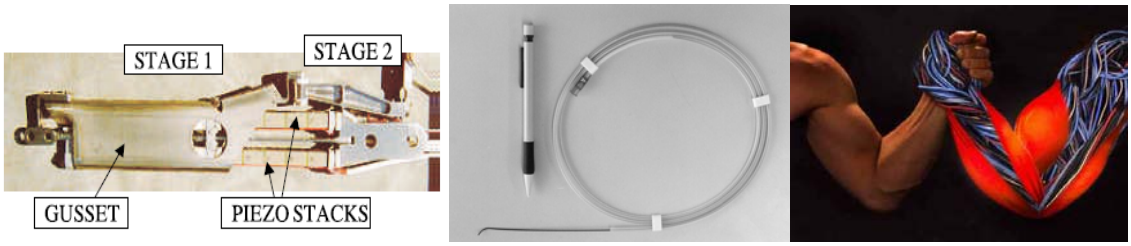

(a) (b) (c)

Figure 1. Present Smart Materials 1.
(a) Piezoelectric materials [18].
(b) Shape memory alloys [23].
(c) Potential application for EAPs in biomimetics [27].

For another example, Ni-Ti alloys, which are one of shape memory alloys (SMAs) groups, have contributed to the development of medical applications as actuators. Such a technological trend stimulated invention of electric-active polymers (EAPs) in 1980s. Controlled by electric signals, EAPs have been one of the technological

breakthroughs in fields such as biomimetic applications as shown in Figure 1. However, EAPs have a limit of controllability in that EAP require physical connections for electric inputs. It means that EAPs must be restricted to control their behavior. To overcome its limit, it is possible to adopt a concept of magnetic materials and thus ferrogels were proposed in this research.

1.2. Introduction of Ferrogels.

A ferrogel is an intelligent magnetic field sensitive gel which is generally comprised of a chemically cross-linked polymer network swollen by a ferrofluid which is a colloidal dispersion of mono-domain magnetic particles [28]. Unlike EAPs, a ferrogel changes its physical behaviors by applying a magnetic field which is a remote control input without any physical connection with the sample. Such an advantage of ferrogels can be a great value in the industries which require non-contacts between a smart material and control input. Simply put, it can be analogized that it is much safer to use a MRI instrument than insert an endoscope into human organs for medical inspection. Likewise, it is certain that characterization and optimization of ferrogel behaviors can be a technical breakthrough in the engineering fields as well as medical applications.

Of course, other smart magnetic materials have been applied in the variety of industrial fields. For instance, magneto-strictive materials such as Terfenol-D and ferromagnetic shape memory alloys (FSMAs) can also be controlled by a magnetic field as described in Figure 2. However, the difference between those materials and ferrogels is a range of stiffness because they have been considered as high modulus magnetic materials, while ferrogels are low-modulus magnetic materials. Among

low-modulus magnetic materials, there are Magneto-Rheological (MR) Fluids and Magneto-Rheological Elastomers (MRE) which are shown in Figure 2. They change their viscosity or modulus when they are exposed to magnetic fields, respectively. Comparing with those two smart magnetic materials, ferrogels show a differentiation because it focuses on actuator behaviors controlled by a magnetic field rather than viscosity and modulus changes.

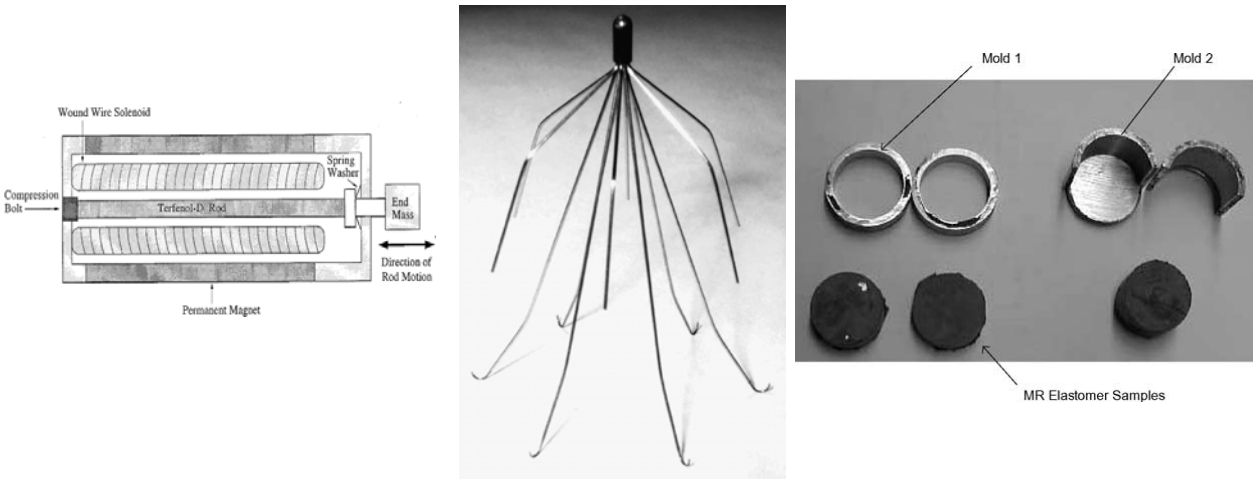

(a) (b) (c)

Figure 2. Present Smart Materials 2.
(a) Terfenol-D magnetostrictive transducer [22].
(b) The recovery filter system [25].
(c) Magneto-rheological elastomer (MRE) samples [26].

In the case of ferrogels, previous work has shown a lot of possibilities. Zrinyi studied ferrogel's behavior when it is exposed to non-uniform magnetic fields by both theoretical and experimental methods in 1997 [28]. In 1999, Mitsumata introduced a new method of making ferrogels using magnetic fluids instead of iron powders [29]. The physical crosslinking method was introduced by Hernández and Ramanujan [30] [31]. Liu showed that ferrogels obtained from Gelatin instead of PVA can be used

for drug delivery system, while Ramanujan focused on the elongation with long cylinder-shaped ferrogels in 2006 [32] [31]. Based on the information in papers about ferrogels as mentioned above, the importance of performing a comparison between the two cross-linking methods arose. Since many of the promising applications of ferrogels involve their strain ability and actuator behavior, it was also important to characterize their mechanical properties. Three types of measurements were selected; free strain tests, loading tests, and time rate tests.

In the case of materials for sample preparation, PVA and iron powders ($Fe(CO)_5$) were selected to produce ferrogels. In general, PVA is a polymer which is widely used for industrial, pharmaceutical, and biomedical applications because of its high biocompatibility [30]. In this research, PVA serves as the main material to analyze and prepare the samples, which are ferrogels. To obtain ferrogels, two methods were used in this research; Freeze-Thaw Cycles (FTC) and Cross-linking with sodium tetraborate. The goal of this work is to analyze mechanical properties of ferrogels, which consist of PVA and iron powders as a main material, such as strength, elongation, and modulus. Secondly, it is to compare the two types of ferrogel crosslinking with FTC and chemical methods..

Chapter 2. BACKGROUND AND LITERATURE REVIEW

Smart Materials.

In recent decades, as science and technology in the materials field have been developed, smart materials have been introduced and improved throughout a lot of industries. Smart materials are defined as materials which have one or more their properties controlled by external stimuli such as magnetic fields, temperature, pH, or stress. They can be applied as active materials for actuators and sensors. Each individual type of smart material has a unique controllable property such as viscosity, conductivity, and external size. Four common types of smart materials are discussed in the following sections: Piezoelectric materials, Shape Memory Alloys (SMAs), Electro-Active Polymers (EAPs), and Magnetic materials.

2.1. Piezoelectric Materials.

Piezoelectricity is defined as the generation of electricity in response to an applied force such as compression, twist, or bending. Reversely, a piezoelectric material also exhibits its deformation as a result of an applied voltage. Simply put, when mechanical stress is applied to a piezoelectric material as an input, the material generates electricity or electric polarity as an output, and vice versa.

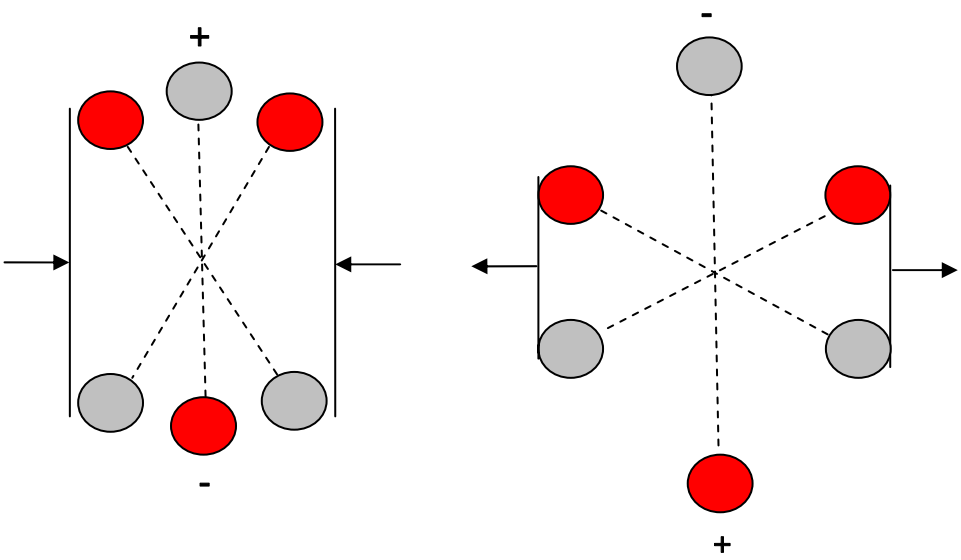

Figure 3. Piezoelectric Effect. (a) Compression (b) Tension [11].
(● : Silicon Atom, Positive, ○ : Oxygen Atom, Negative.)

As can be shown in Figure 3 above, the unit cell of crystal silicon dioxide (SiO_2), a piezoelectric material, is used to explain the piezoelectric effect [11]. The compression and the tension of mechanical stress enable the piezoelectric material to be polarized and generate electrical currents [11]. When SiO_2 is compressed with an external stress, positive silicon atoms are aligned in the direction perpendicular to that of the stress. As a result, the piezoelectric material is polarized due to the driven positive and negative atoms. The direction of electric charges also depends on the types of mechanical stress. This phenomenon was discovered by Pierre and Jacques Curie in 1880 and called as the piezoelectric effect [9].

An example of an application for piezoelectric materials using the piezoelectric effect is the airbag sensor in a vehicle, which sends electric charge deploying the airbag when they sense the force of an impact on the vehicle [2] as described in Figure 4.

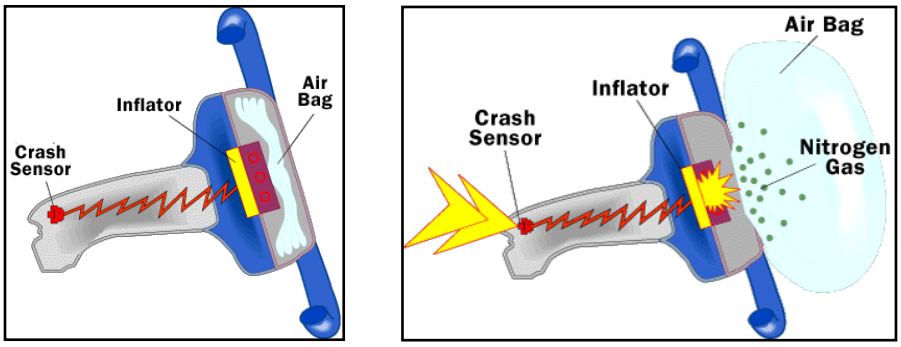

Figure 4. Schematic of an air bag [2].

For piezoelectric actuator, first, the electromechanical effect should be described to introduce applications of piezoelectric actuators. The electromechanical effect is the relationship between a mechanical stress and an electrical current in the material. When a power source is off, which means there is no electrical current, charges in the material are canceled and thus the material keeps its original shape. If an electrical current is applied to the material, the atoms in the material are driven to each side, which is positive and negative. The polarized material can achieve bulk deformation.

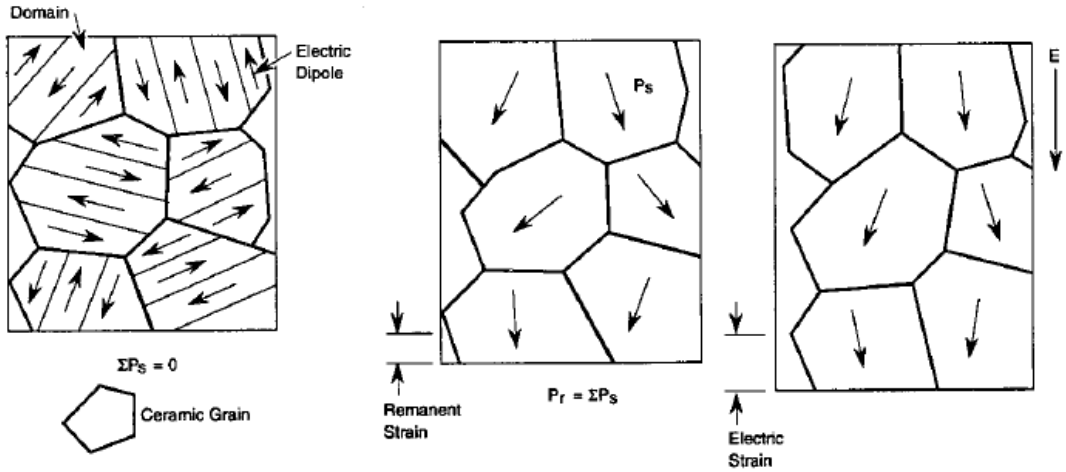

Figure 5. The behavior of Piezoceramic material. (a) Non-polarized state, (b) Polarized state, (c) Electric applied after poling [9]

Secondly, Figure 5 explains the behavior of piezoceramic materials with electric dipoles. As shown in Figure 5(a), the domains in the piezoceramic material are randomly oriented and thus the net external electric dipole is zero when no electric field is applied; $\sum P_s = 0$ [9]. If an electric field, which is poling, is applied to the piezoceramic material, the united dipoles in each domain align in the direction of electric field. However, it is not possible to be perfectly aligned in the direction of the field because there is the random original orientation of domains [9]. When the voltage is removed, the domains do not entirely return to their original positions, and the material remains partially polarized. As a result, the strain resulted from the partial polarization as shown in Figure 5(b) [9]. After such a poling, if electric field is applied, the material elongates in the direction of the field. It means that the material can convert mechanical energy into electrical energy vice and versa as shown in Figure 5(c).

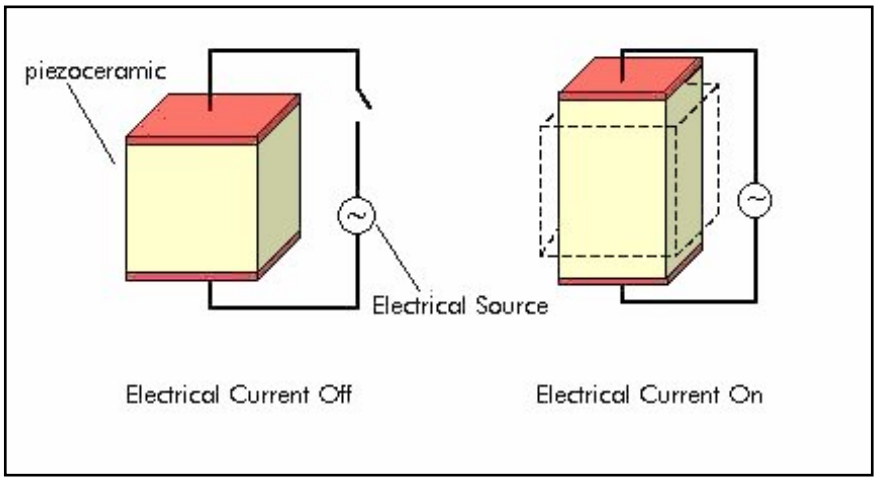

Figure 6. The schematic of the Electromechanical Effect [4].
(a) Electrical Current Off. (b) Electrical Current On.

According to the article of "Piezoelectric Materials" [4], Figure 6 describes the change of the shape in the piezoceramic material. When an electrical current is off, the shape of piezoelectric material does not exhibit any change in its volume. However, when an electrical current is applied to the piezoelectric material, the current changes its shape and enables the material to act as an actuator. The reason why the piezoelectric material exhibits the electromechanical effect is also similar to that of piezoelectric effect. The disadvantage of a piezoelectric material is small strains, which are from 0.1% to 0.2% and up to a 4% change in its volume [9]. Moreover, another drawback of PZT actuators is that a PZT actuator requires a high supply voltage, which is typically 60 and 100 volts [9].

2.2. Shape Memory Alloys (SMAs).

Shape Memory Alloys (SMAs) are metallic materials which exhibit two very unique properties; pseudo-elasticity and the shape memory effect [33]. The SMAs have two stable phases; the low temperature phase called as martensite and the high temperature phase called as austenite as shown in Figure 7. In addition, the martensite can be in one of two crystal structures under unloading or loading; twinned martensite and detwinned martensite, respectively. As one phase of metallic structure, austenite is formed with a Body-Centered Cubic (BCC) structure at high temperature [17]. When the austenite structure is cooled, the alloy exhibits a lattice distortion called as martensite transformation to a Face-Centered Cubic (FCC) structure [17] [34]. The Figure 7 shows general comparisons between martensite and austenite structures.

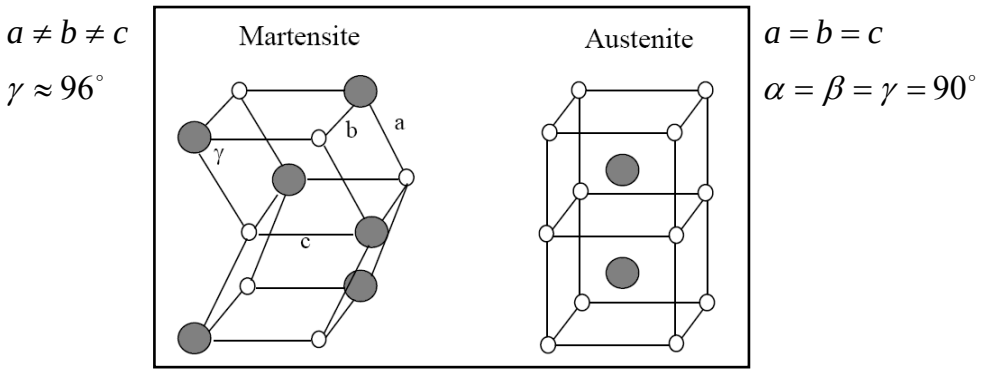

Figure 7. Schematic of Unit cells of NiTi in the martensite and austenite phases [12].

Pseudo-elasticity is defined as a non-linear thermo-elastic deformation of SMA. As can be shown in Figure 8, a green curve stands for a loading path on temperatures and shows that SMA's mechanisms involve large irreversible deformations under low loads due to crystalline detwinning [8]. Initially, SMA is in the austenitic phase around a point A. Then, the transformation and detwinning of the martensitic occurs along the loading path and reaches fully transformed and detwinned martensite phase around a point C. When unloading is applied, the end of the loading path is located in a point E which is in the austenitic phase.

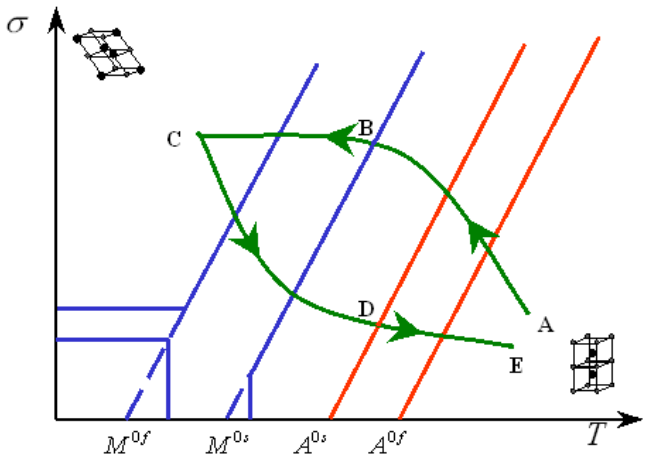

Figure 8. Schematic of a thermo-mechanical loading path demonstrating pseudoelastic behavior of SMAs [8].

For that reason, the SMA exhibits the mechanical behavior similar to the rubber in spite of its metallic characteristics. The shape memory effect can be defined as the ability of SMA to recover its shape into the original shape when the SMA is cooled through a phase transition (see Figure 9). As described in Figure 9, the SMA is capable of changing and recovering its shape upon applications of an external stimulus such as temperature or stress [35]. The Figure 9 also shows that the SMA can convert its shape into a preprogrammed structure in response to change of temperature [17].

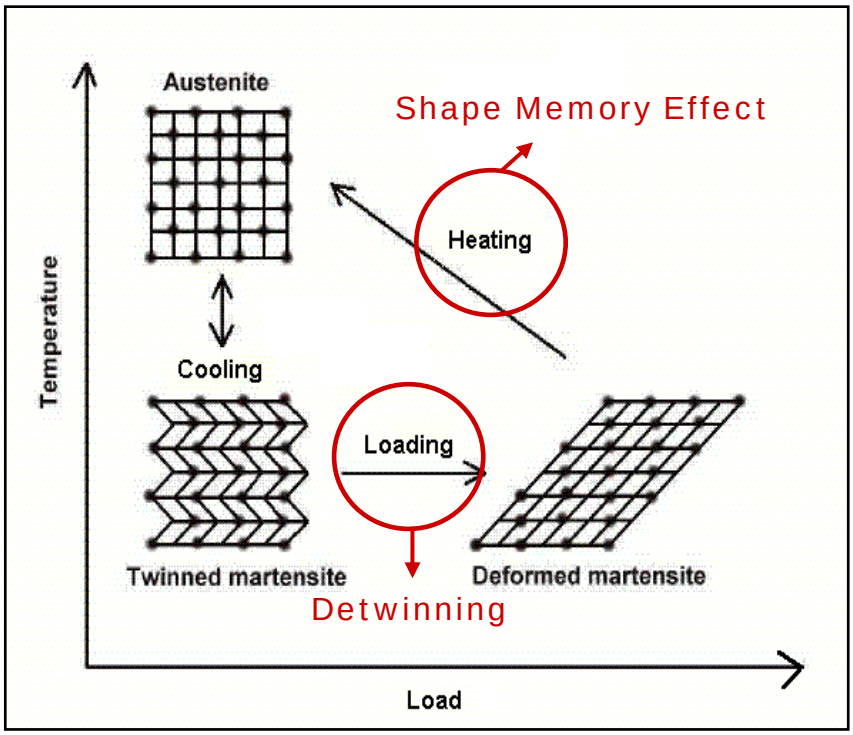

Figure 9. Transformation from the austenite to the martensite phase and shape memory effect [17].

Ni-Ti alloys, a type of SMAs, have been widely utilized for engineering materials since NiTi alloys exhibit great mechanical properties. Its applications of SMA include both medical and industrial applications. Owing to its high biocompatibility, micro staples or catheters and implants such as coronary stents are made out of Ni-Ti

SMAs [16]. As can be shown Figure 10, when a staple is cooled to -50°C, its shape is mechanically changed. Plus, in case of industrial applications of SMAs, Ni-Ti eyeglass and cellular phone antenna were introduced and mass-produced using their superelastic characteristics. Even, the same is true for wires for women underclothes [36].

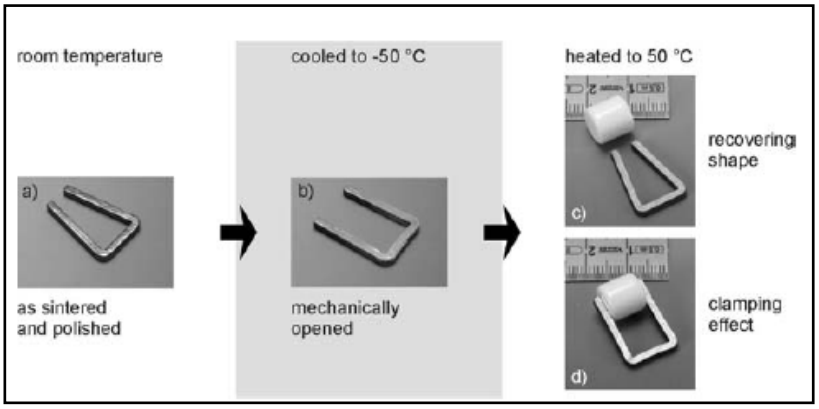

Figure 10. The behavior of the staple during a cooling-heating cycle [16].

2.3. Electro-Active Polymers (EAPs).

Comparing with SMAs, Electro-Active Polymers (EAPs) have a difference because of the fact that such a polymer can be controlled by electric signals. EAPs could be also differentiated from PZT because EAPs have a very low modulus and thus strain much more than PZTs; EAPs achieve longitudinal deformations at the range from 4-350% [19]. Because EAPs exhibit a macro-scale deformation overcoming large forces, they can be also used for artificial muscles and robotics applications [37]. There are two classification of EAPs based on the types of control inputs; electric EAPs and ionic EAPs.

2.3.1. Electric EAPs.

Many types of polymers with low elastic modulus and high dielectric constant have been used to induce large actuation strain by subjecting the material to an electrostatic field. Electric EAP actuators require large electric fields and can produce large strain levels [19]. A dielectric EAP actuator, one of electric EAPs, can be used as a compliant capacitor where the polymer is inserted between two compliant electrodes as described in Figure 11. When a capacitor is charged, a pressure known as Maxwell pressure is applied between the two electrodes.

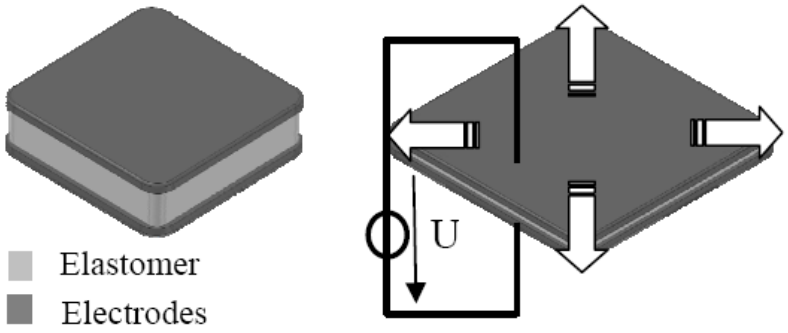

Figure 11. Dielectric EAP principle [24].

Maxwell pressure is created when a capacitor is charged. The pressure results in the stretch of the polymers. As a result, the dielectric polymer as well as the electrodes would expand in the area as described in Figure 11. The Figure 11 also shows that such a stretch reduces electrical energy and also decreases the thickness of the elastomer [24]. The reduction in electrical energy is balanced by an increase in elastic mechanical energy, which is the mechanical work output [24].

2.3.2. Ionic EAPs.

Polymers containing ions have been referred to as ionic polymers. An ionic polymer is defined as the material containing a loosely collected arrangement of charged atoms, which are ions, bonded to the molecular 'backbone' [19]. When a voltage across an ionic polymer is applied, the polymer produces mechanical deformation, vice and versa. Such a deformation would cause the migration of electrons to electric field as shown in Figure 12. As a result, ionic materials can be used as electromechanical sensors and actuators. Owing to such a principle of ionic EPAs, the main advantage of ionic EAPs is the low voltage required for actuation.

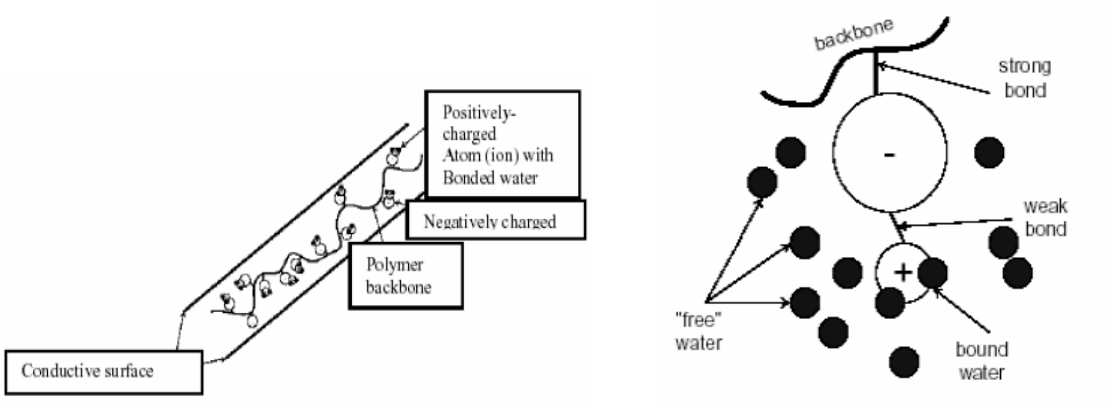

Figure 12. The operating principle of ionic EAPs actuator [19] .

However, there are some limitations, which ionic EAPs have, when they are compared with electric EAPs. Most of ionic EAPs could not hold strain under DC voltage, while electric EAPs can be made to hold the induced displacement under DC voltage [19]. Moreover, electric EAPs show great performances on mechanical energy density than ionic EAPs as well as can be rapidly activated in air without any constraints [19]. However, the main disadvantage of electric EAPs is the high

amount of voltage to be activated [19]. In general, there are still needs to produce EAPs which have greater force and efficiency.

2.4. Smart Magnetic Materials.

Though the earliest observation of magnetism can be traced back to the Greek philosopher Thales in the 6th century B.C., the modern developments of magnetism were begun by "De Magnete", which is the first systematic experiment paper published in 1600 [38]. Similar to the deformation of SMA in response to external stress and temperature changes which is discussed above, a smart magnetic material is controlled by an applied magnetic field [39]. For the purpose of discussing smart magnetic materials, we will divide them into two different types; high and low modulus smart magnetic materials.

2.4.1. High Modulus Smart Magnetic Materials.

High modulus smart magnetic materials are generally metallic alloys with properties which are dependent on a magnetic field. Exanples of these include:

- Magnetostrictive (Terfenol & Galfenol)
  : convert magnetic energy into kinetic energy.
- Ferromagnetic Shape Memory Alloys (FSMAs)
  : Same as magnetostrictives but show a shape memory effect.
- Magnetoresistive and Magnetocaloric
  : generate change in resistance or temperature by magnetic fields.

2.4.1.1. Magnetostrictive (Terfenol-D & Galfenol).

Magnetostriction is a property to deform the shape of the magnetostrictive material due to applied magnetic fields [40]. Simply put, magnetostrictive materials are defined as materials which undergo a change in their shapes as a result of changes in the magnetization state of the materials and convert magnetic energy into kinetic energy. A few examples of magnetostrictive materials are cobalt, Terfenol-D (Terbium Alloys), and Galfenol [41]. As compared to piezoelectric materials, magnetostrictive materials can serve as actuators at higher temperature and also undergo higher strains.

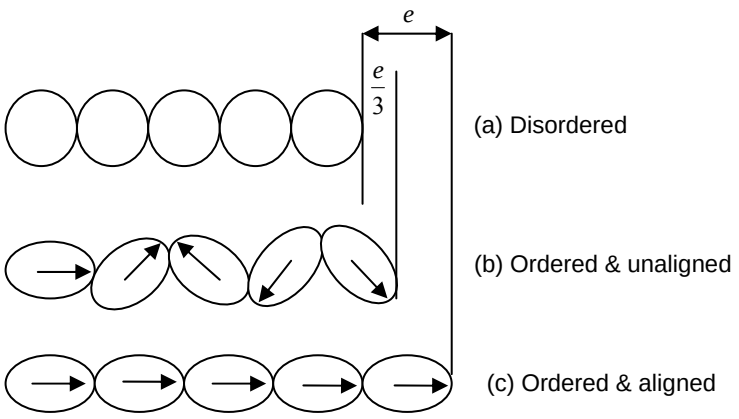

Figure 13. Schematic Diagram of the Magnetostrictive Materials [1].

The mechanism of the magnetostriction can be described in Figure 13 above. Initially, a Ferromagnetic material has disordered magnetic moments, which are paramagnetic in Figure 13 (a). When it is cooled through its Curie point, those moments become ordered over volumes containing large numbers of atoms as shown in Figure 13 (b) [1]. When a field is applied, those magnetic moments become aligned like Figure 13 (c) and thus the magnetostrictive material becomes magnetized. The strain e is caused by ordered magnetic moments with alignments of magnetic

moments in the magnetostrictive material.

As an intermetallic compound, Terfenol-D has been widely adopted for magnetostrictive applications. Especially, Terfenol-D operates with wide range of temperatures. It is because Terfenol-D has a Curie temperature, which is the temperature above which magnetization is zero due to heating, as high as $357\,^{o}C$ [42]. Plus, Terfenol-D requires low magnetic field by balancing the ratio of Terbium and Dysprosium which are choice materials for Terfenol-D [42] [43]. In case of strain mechanisms with Terfenol-D, it can show strains on the order of $1000\times10^{-6}\,m/m$ (1000 ppm) [44] [45]. Despite its low tensile strength, Terfenol-D has been used as a material for transducers in harmonics applications [43] [46] . Therefore, Terfenol-D is a good option for applications which require high magnetostrcition and large blocked force. However, there are still several drawbacks in using Terfenol-D. Due to its high brittleness, Terfenol-D can develop cracking after prolonged periods of actuation. In addition, Terfenol-D requires high levels of input power or electromagnetic field for its maximum strain as shown in Table 1 [45].

$Fe_{100-x}Ga_x$ (galfenol) has "mechanical strength and malleability with a high relative permeability and reduced cost of fabrication [47]". Since Ga in galfenol produces the highest magnetostriction in the group of alloys [47] and excellent mechanical properties [43], galfenol thin film cantilevers have been successfully installed into MEMS applications [43]. In other words, galfenol is easy to use without breaking owing to its flexibility, while Terfenol-D is not acceptable enough to apply in some applications due to its high brittleness. However, the main drawback of Galfenol is that its magnetostriction strain is about 300 ppm, which is smaller thatn that of Terfenol-D as shown in Table 1[45].

Table 1. Comparison of Terfenol-D and Galfenol Material Properties [45].
(* Varies with stress and applied field.)

Magnetostrictive Material Properties		
	Terfenol-D	**Galfenol**
Length	2"	2"
Diameter	0.25"	0.25"
Magnetic Permeability	3-10	300
Free Strain	1000 ppm	300 ppm
Required Field for Maximum Strain	80 [kA/m]	25 [kA/m]
Young's Modulus	10-100 [GPa]*	30-57 [Gpa]*
Temperature Sensitivity	20% loss at 80 $^{\circ}C$	10% loss at 80 $^{\circ}C$
Robustness	Very Brittle	Machinable

2.4.1.2. Ferromagnetic Shape Memory Alloys (FSMAs).

Ferromagnetic Shape Memory Alloys (FSMAs) were identified by Ullakko at MIT in 1996 [48]. FSMAs can show a shape memory effect controllable by an applied magnetic field, while common SMAs generally respond to the external stimuli such as temperature changes or mechanical stress [49] [50]. Ni-Mn-Ga alloys have been the focus of FSMA research because they have shown the most promise as ferromagnetic shape memory alloys [48]. These materials are candidates for biomedical applications such as human implants [50]. FSMA research has also been done with alloys in the Ni-Fe-Ga system and the Ni-Mn-Fe-Ga system as well as Fe-Pt, Co-Ni-Al, and Co-Ni-Ga [51].

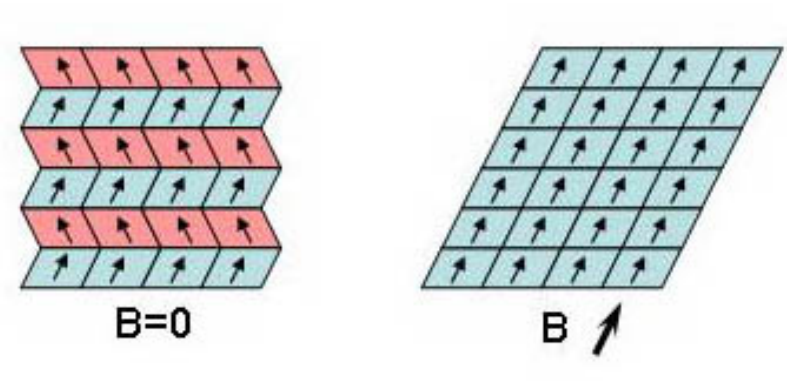

Figure 14. Principle of the Ferromagnetic Shape Memory Effect [5].

FSMAs have a large magnetic anisotropy which differentiates FSMAs from other magnetic materials such as magnetostrictives. When the magnetic anisotropy energy is large enough, the physical orientation of the unit cells is changed by the alignment of magnetization vectors with the applied field. As a result, FSMAs can create strains due to its transformed orientation as shown in Figure 14 [5]. In other words, in ferromagnetic shape memory materials, the magnetic moments of the twin variants play an important role in the deformation process. When a sample is exposed to an external magnetic field in the martensitic phase, the magnetic field tends to realign the magnetic moments along the field. Simultaneously, the variant in a favorable orientation with respect to the field grows resulting in strains as shown Figure 14 [5]; the resulting deformation can be as large as 10 % [5].

2.4.1.3. Others – Magnetoresistive and Magnetocaloric.

Besides magnetostrictive materials and FSMAs, there are magnetoresistive and magnetocaloric materials for high modulus smart magnetic materials. By changing

the magnetic field as an input, magnetoresistive materials generate change in resistance as an output. In general, the electrical resistance of magnetic materials changes when they are magnetized. Most of such a change is an increase in resistance in bulk magnetic materials when electrical currents are paralleled to magnetization, while there is a decrease when the currents are perpendicular to magnetization [1]. They are useful for commercial and military applications such as navigation systems [52]. Recently, magneto résistance has been studied in magnetic multi-layers and this leads to rapid increase in available types of magnetoresistive materials. The applications of magnetoresistive materials are vibration monitoring sensors and transducers [53].

In case of a magnetocaloric material, a temperature change of the material, ΔT, is generated by an applied magnetic field producing a magnetocaloric effect [54]. Magnetocaloric materials such as $Gd_5(Si_{1-x}Ge_x)_4$, $Mn(As_{1-x}Sb_x)$, $MnFe(P_{1-x}As_x)$, and $La(Fe_{13-x}Si_x)$ are usually adopted in the temperature applications like magnetic refrigeration [54].

2.4.2. Low Modulus Smart Magnetic Materials.

Previously, high modulus smart magnetic materials such as magnetostricitive materials and FSMA have been discussed and reviewed. There are also a number of low modulus smart magnetic materials because they are viscoelastic enough to be applicable in the range where high modulus smart magnetic materials can not be adopted. With their viscoelastic properties, they are also controllable by applied magnetic fields and thus are useful for applications which are difficult to adopt stiffer smart magnetic materials. Low modulus smart magnetic materials can be classified

as three types of materials; Magneto-Rheological (MR) Fluids, Magneto-Rheological (MR) Elastomers, and Ferrogels.

2.4.2.1. Magneto-Rheological (MR) Fluids.

Magnetorheological (MR) fluid is a fluid with a viscosity which is controllable by a magnetic field [14] [55]. Coined by Eugene Bingham in 1920, the term of "Rheology" is defined as the physical property which describes the study of the deformation and flow of matter in response to external stress. Simply put, MR fluid's rheological property is defined as a mechanical behavior of reversible and instantaneous change between a free-flowing liquid state and a semi-solid state by controlling a magnetic field [55]. In general, commercial MR fluids are colloidal fluids with micro-scale (1-10 μm) paramagnetic particles [14]. Paramagnetism is defined as atomic behavior with randomly oriented magnetic moments [38].

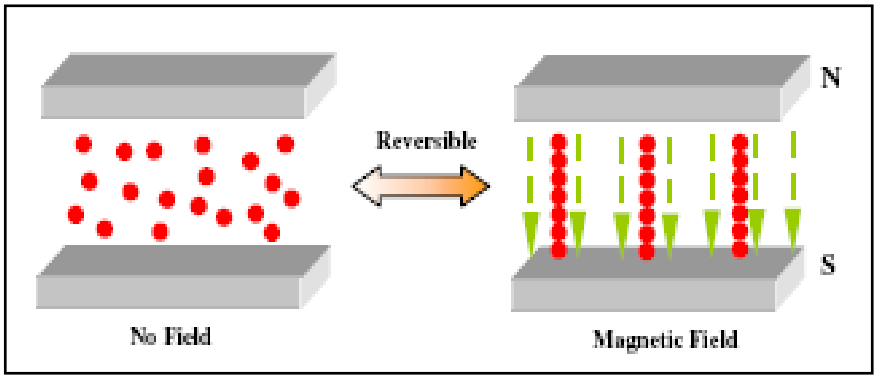

Figure 15. Schematic of the MR effect [14].

As described in Figure 15 above, when no magnetic field is applied, particles in MR fluids are randomly positioned. When exposed to a magnetic field, particles in MR fluid exhibit paramagnetism by alignments of atomic moments [14]. In the

process, the original particles become magnetized and thus acquire dipole moments which are able to form chains in the field direction [14]. As a result, the structure of MR fluids in a magnetic field causes the attraction between particles which leads to high viscosity in MR fluids.

Figure 16. MR fluids. (a) Non-magnetic filed (b) Applied to a magnetic field [7].

As shown in Figure 16, MR fluid is liquid-state which consists of iron particles suspended in specific oil in zero-magnetic field. When a magnetic field is applied, the MR material changes to nearly solid-state quickly. For that reason, smart MR materials are widely used for engineering applications such as dampers against vibration [14], clutches, or valves [55].

2.4.2.2. Magneto-Rheological Elastomers (MREs).

Magneto-Rheological Elastomers (MREs) are the solid state equivalents of MR fluids where magnetic particles are suspended in an elastomer matrix [56]. The rheological properties of MREs are a mechanical behavior of semi-solid materials, while that of MR fluids are a mechanical behavior of free-flowing fluids. The stiffness of MREs can be controlled continuously, rapidly, and reversibly by an

applied magnetic field. The mechanism in MR elastomers can be explained with magnetic particles with crosslinking. The controllability in response to an applied magnetic field in MR elastomers become achieved with uniformly embedded magnetic particles into a crosslinked polymeric rubber [57]. They consist of micro-scale magnetically polarisable particles in an elastomer matrix. Similarly with MR fluids, the particle size generally varies from 0.1 to 10 μm [56]. Larger particles in MR elastomers enable them to obtain stable and high magnetization [56].

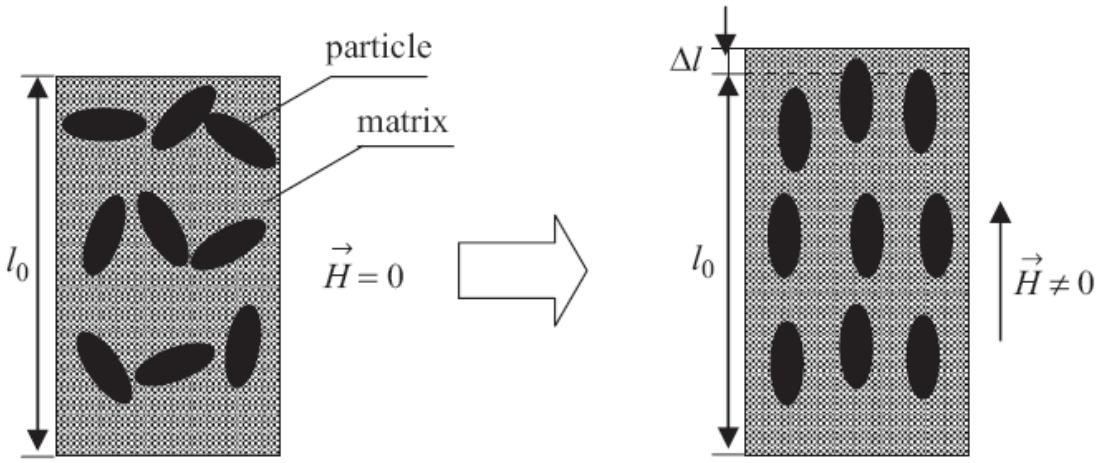

Figure 17. The schematic of mechanism of MRE with interaction between magnetic particles and matrix under magnetic fields [20].

Figure 17 shows the mechanism of MREs under magnetic fields applied. Similar to Figure 15, there are randomly distributed magnetic particles when no magnetic field is applied. However, it is important to note that the particles in the MREs are physically locked into place by the elastomer and thus they are allowed to rotate but not to move. Regarded as the shape of ellipse, each magnetic particle is magnetized when a magnetic field is applied and simultaneously magnetic dipole moments are induced. Such a phenomenon results in the rotation from random to the magnetization direction of particles. As shown in Figure 17, the rotation of particles

enables the stiffness of MREs to be increased as well as the strain to be created [20]. Ginder found that MREs, which contain magnetic particles in natural rubber, show a 30% to 40% maximum change in modulus or stiffness under a saturating magnetic field [58]. These considerable stiffness changes are large enough to be installed into composites in variable stiffness device.

However, there are still disadvantages of MREs when they are applied to industries; small strains and the limited capability. Guan observed that MREs with 27% of magnetic particles exhibits the maximum strain of 183ppm under the maximum magnetic field of 636 [kA/m] [20]. MRE's strains due to the magnetic field are as large as piezoelectric ceramics. However, compared with magnetostrictive materials such as Terfenol-D, the strain value is smaller than that of Terfenol-D; the strain is of Terfenol-D is about 1000 ppm under lower magnetic fields applied. The main drawback of typical MREs is the limited capability of a MRE damper due to numbers of oscillatory cycles and increased frequency but there are still possibilities to improve MREs [59]. In the engineering or automotive fields, MR elastomers are widely adopted for shock and vibration absorbers [60]. Plus, in biomedical applications, a MR elastomer damper was used in a prosthetic knee was introduced in 2000 by Carlson and Sproston [60].

2.4.2.3. Ferrogel.

Smart gels can be defined as a crosslinked polymer networks swollen with water [31] which is responsive to external stimuli [32]. As previously stated in the introduction of ferrogels, a ferrogel have an advantage that a remote control input without any physical connection is used to create its behavior, while EAPs require

physical connections. Such a promising advantage of ferrogels could be outstanding value in the industries which require non-contacts between a smart material and control input. Among types of smart materials mentioned above, MR elastomers and ferrogels can be involved in the category of smart magnetic sensitive gels. In this study, ferrogels with Polyvinyl Alcohol (PVA), which is a gelating substance, are discussed while reviewing recent studies on smart magnetic materials such as ferrogels. First, studies which adopted PVA for gel preparation will be compared and discussed. Next, Freeze-Thaw Cycles and Chemical Crosslinking methods will be introduced and compared for manufacture of gels.

In recent years, magnetic responsive gels or ferrogels have become an interesting subject of study for several research groups. Polymer gels are a class of macromolecular networks with unique properties [13]. In 1964, Joseph and Ronald introduced and published a field of ferrohydrodynamics [61]. As one type of ferrohydrodynamic materials, ferrogels, which were gelated, not be a fluid state with magnetic properties, have been shown and developed by engineers and scientists.

Ferrogels can be considered as a new class of magneto-controlled elastic materials which are produced with chemical crosslinking of polymer networks with ferrofluids [62]. A typical size of particles in ferrogels is about $10\,nm$, while that of particles in a MR elastomer is microscale as mentioned above [28]. Such nanoscale particles result in the superparamagnetism of ferrogels. Super-paramagnetism is defined as a smaller length-scale magnetic behavior of ferrogels over a larger range of temperatures [28].

Ferrogels have been researched for biomedical applications owing to their great biocompatibility [61]. In the past ten years, there have been successful outcomes related with ferrogels. Especially, Zrinyi studied the shape transition in ferrogels

when they were exposed to non-uniform magnetic field in 1997 [28]. In the study, ferrogel samples were prepared by synthesizing Polyvinyl Alcohol (PVA) with iron powders (Fe_3O_4) as well as $HClO_4$ and Glutardialdehyde (GDA) serving as a stabilizer and a checmial cross-linker, respectively. Modeled by theoretical and experimental methods, ferrogels were characterized with their elastic behaviors and unidirectional magneto-elasticity.

In 1999, Mitsumata adopted magnetic fluids (W-40 Taiho Industry) as magnetic particles instead of iron powders, while other types of agents were same as Zrinyi did [63]. Another difference was that Mitsumata's samples were shaped as sheets (10x10x5mm) and the cylindrical samples were used by Zrinyi. In the paper, Mitsumata found that the compressive modulus of ferrogels was increased when a magnetic field applied and the mean change in modulus saturated above 2 kOe [63]. It was also shown that the mean and maximum change in modulus at 4 kOe was 31 and 71 Pa corresponding to 19% and 46% of increase of that without a magnetic field, respectively [63]. Then, the change in modulus was analyzed theoretically using a non-Hookean stress-strain theory.

According to the paper published by Zrinyi in 2000, Poly (N-isopropylacrylamide) (NIPA) hydrogel beads with magnetic particles was prepared and their sensitivity was measured by applying a magnetic field as shown in Figure 18 [13]. Besides, a cylindrical sample with 0.72 g of PVA and 0.96 g of magnetite nanoparticles, whose overall volume is $12\,cm^3$, was used for loading tests [13]. In the result of the paper, Zrinyi observed that the maximum of mechanical work done by a ferrogel was about 5 mJ under 12 g of the load and 300 mT of a magnetic field [13].

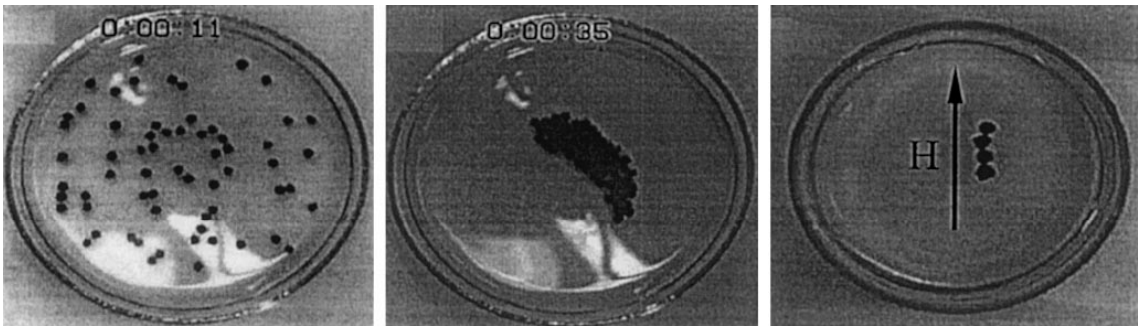

Figure 18. Influence of uniform and nonuniform magnetic fields on bead gels [13].
(a) no magnetic field is applied,
(b) non-uniform magnetic field is created by a permanent magnet,
(c) homogeneous magnetic field. (H: Magnetic field.)

After Raikher contributed to the ferrogel susceptibility in 2001 [64], there were active research for ferrogels by a lot of contributers such as Chatterjee [65], Collin [66], Galicia [67], and Jarkova [62] in 2003. Especially, Galicia focused on measuring ferrogel elasticity over a large range scales with experimental approaches [67]. Before 2003, chemical crosslinking method was mainly used to produce gels. Beginning in 2004, the physical crosslinking method was attempted by Hernández and Ramanujan [30] [31]. Moreover, it is distinguished that Hernández compared visco-elastic properties of PVA hydrogels with those of PVA ferrogels. Hernández found that the formation of crystalline zones or cooperative hydrogen bonds of ferrogels start at the transition temperature, which is $35.5\,^{\circ}C$ [30]. Moreover, Hernández described that the increase of freezing-thawing cycles enable a ferrogel to show the higher viscoelastic storage modulus [30].

In the paper of Liu (2006), it is distinctive that ferrogels obtained from Gelatin instead of PVA was used for drug delivery system [32]. Ramanujan measured elongation with long cylinder-shaped ferrogels, which include PVA with a weight composition of 23:100 in water and from Fe_3O_4 (1wt.% to 10wt.%). The size of a

ferrogel was 4.5mm of diameter [31]. In the paper, Ramanujan found that the maximum deflection of a ferrogel due to magnetic field strength is about 47 [mm] using a sample with 10 wt.% of Fe_3O_4 [31]. Moreover, Ramanujan showed that the tensile strain of a ferrogel exhibited the elongation of 150% when 1 [MPa] of a tensile stress was applied [31].

For this research, it is important which type and what materials of ferrogels should be adopted to characterize its actuator behaviors. Typically, PVA or gelatin has been mainly used to produce ferrogel samples according to the current trends, while two types of crosslinking methods were described; chemical and physical methods. However, gelatin was excluded from the sample preparation before experimental tests start. It was because gelatin was easily contaminated within three days when a ferrogel with gelatin was put at the room temperature. For that reason, PVA was considered as a material which is crosslinked with two methods mentioned above. When it comes to a physical crosslinking method, the Freeze-Thaw Cycle (FTC) method, which Hernández and Ramanujan used, was chosen but was optimized to reduce the production time; details will be described in the next chapter. As a chemical crosslinker, sodium tetraborate powders were selected because their high chemical attraction with PVA. To help understand characterization of ferrogels developed, there are two tables below. Table 2 shows the classification of smart magnetic materials which were discussed above. Plus, Table 3 shows the history of ferrogels preparation and trends.

Table 2. The classification of Smart Magnetic Materials.

Type		Magnetic Property	Example
High Modulus	Magnetostrictive	Magnetic energy into kinetic energy.	Terfenol / Galfenol
	FSMA	SMA with ferromagnetism	Ni-Mn-Ga alloys
	Magnetoresistive	generates change in resistance	Fe/Cr Multilayers
	Magnetocaloric	Temperature change of the material.	$Gd_5 / Mn / MnFe / La$ Alloys
Low Modulus	MR Fluid	Variable viscosity dependent on magnetic field	Magnetorheological Dampers
	MR Elastomer	Modulus controlled by magnetic field	Active Dampers
	Ferrogel	Active magnetic field-sensitive gel	PVA / Gelatin Gel

Table 3. History of ferrogel preparations and technical trends.

Author	Year	Materials	Method	Uniqueness
Zrinyi	1997 T►E	Fe_3O_4, PVA, GA (GDA)	Chemical Crosslinking $HClO_4$ as a stabilizer.	Cylindrical D:1-2cm L:10-20cm
Mitsumata	1999 T►E	PVA, Magnetic Fluid . GA(GDA) – 2 mol%	Chemical Crosslinking $HClO_4$ as a stabilizer.	Sheet-shaped gel (10x10x5mm)
Zrinyi	2000 S	NIPA & PVA	Chemical Crosslinking	Bead gels.
Raikher	2001 T	-	Single Domain Particles Frozen-In. Rheological Maxwell Model Single Relaxation Time	Measured Magnetic Susceptibilities.
Chatterjee	2003 E	Fe_2O_3 Hydroxy Propyl Cellulose (HPC) Sodium Hydroxide Ferrous Chloride Ferric Chloride Nitric Acid Cetyldimethylethyl-ammonium Bromide (CTAB) Divinyl Sulphone	Synthesis of Fe_2O_3 1. Precipitation of particles within a polymeric matrix before or after crosslinking. 2. Mix magnetic particles with a polymer (Crosslinking).	Nanoscale The magnetic susceptibilities measured by a superconducting Quantum interference device magnetometer.
Collin	2003 E	M-300 (Sigma-Hi-Chemical) PVA, GA(GDA), HCl	Chemical Crosslinking M-300 synthesized with PVA.	Optical properties of thin samples.
Galicia	2003 S►E	Citrate-Coated Particles. (CitMF) Ammonium Persulfate (APS) N'-Methylene-Bis-Acrylamide (BA) Acrylamide Monomer (AM) Tri-Sodium Citrate Electrolyte(Na_3Cit)	Chemical Crosslinking with BA. APS as an initiator. Mixed CitMF with AM. (+APS+ Na_3Cit)	Elasticity measured over a large range scales. (Macro/Micro/Nano)
Jarkova	2003 T	Isotropic Ferrogel. (Nanoscale)	Statics, Thermodynamics, Equilibrium, Dynamics	Hooke's Law Maxwell Equations
Hernández	2004 E	PVA Polystyrene Sulfonic Acid Sodium Salt. (DOWEX 50W4-200) $CoFe_2O_4$	Ferrofluids from $CoFe_2O_4$. PVA hyhdrogel from FTC (Physical Crosslinking). Ferrofluids + PVA gel.	Comparison with PVA hydrogel and ferrogel.
Liu	2006 E	Gelatin Fe_3O_4 Genipin (GP)	Chemical Crosslinking with GP. Gelatin (15wt.%)+ Fe_3O_4 (4 wt.%).	Drug Release system
Ramanujan	2006 E	PVA Fe_3O_4	Physical Crosslinking with FTC. PVA + Fe_3O_4	Cylindrical gel. (D:4.5 mm) Elongation.

(Modeling: T-Tehological, E-Experimental, S-Summary.)

Chapter 3. MATERIALS AND METHODS

As materials used in this research, Polyvinyl alcohol (PVA), Carbonyl Iron Powder (CIP, $Fe(CO)_5$), and Sodium Tetra-borate ($Na_2B_4O_7 \cdot 10(H_2O)$) were adopted. These samples were synthesized using either chemical or physical crosslinking methods for samples containing PVA of 4, 8, and 12 wt% and CIP of 1, 5, and 10 wt%. When it comes to crosslinking methods, freeze-thaw cycles (FTC) method and Sodium Tetra-borate (borax) as the physical method and the chemical crosslinker, respectively. After synthesis, samples were then tested for free strain and strain under loads of up to 4 times their weight by exposing them of fields from between 0.2 and 0.25T.

3.1. Materials.

In this research, polyvinyl alcohol (PVA) was used as the matrix material with a filler of iron powder. With polymer chains, PVA can hold iron powder in the chains. Carbonyl Iron Powder (CIP, $Fe(CO)_5$) serves as magnetic particles, which respond to magnetic fields. In other words, CIP enables samples to achieve actuator behavior driven by magnetic fields. Sodium Tetra-borate ($Na_2B_4O_7 \cdot 10(H_2O)$), which is the main ingredient in Borax, was adopted as a chemical crosslinker for some samples.

3.1.1. Polyvinyl Alcohol (PVA).

Introduced by Hermann and Haehnel in 1924, PVA has been obtained from "hydrolyzing polyvinyl acetate in ethanol with potassium hydroxide." [68] With a

chemical structure in Figure 19, the hydrogen bonding between hydroxyl groups enables PVA to exhibit its unique chemical and physical properties [69]. For example, PVA can be easily dissolved and gelated with water owing to its high water solubility as a result of the hydrogen bonding [69]. When PVA is produced into thin-film, it has emulsifying and adhesive properties. Plus, PVA has high biocompatibility as well as tensile strength and flexibility. These properties have been found to be dependent on the ratio of PVA and water [69].

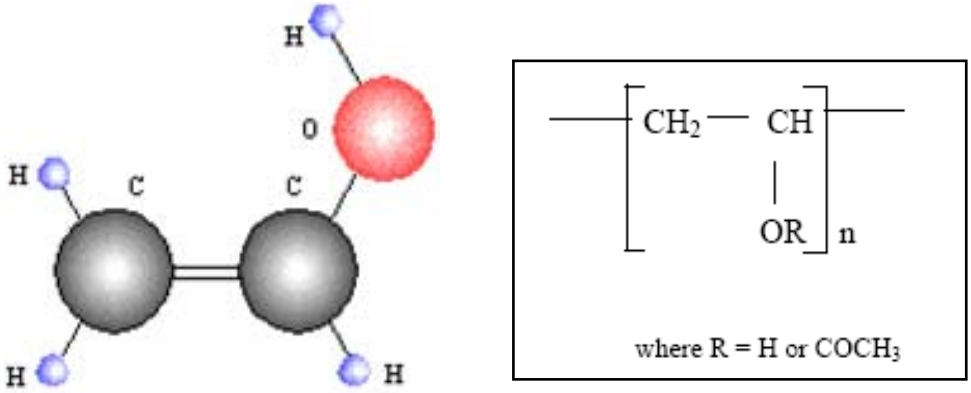

Figure 19. Chemical Structure of Polyvinyl Alcohol (PVA) [3].

3.1.2. Carbonyl Iron Powder (CIP, $Fe(CO)_5$)

Carbonyl iron powder (CIP), which is also called ferronyl iron powder, is chemically decomposed iron penta-carbonyl. In this study, micro iron powders (Carbonyl powder) obtained from ISP technologies Inc. were adopted as magnetic particles. As shown in Figure 20 (b) , the iron particles are uniform gray microscopic spheres when it is photographed with SEM (Scanning Electron Microscope). Carbonyl iron powder is composed of very fine spherical particles with the size of 5 μm to 10 μm diameter. Moreover, there are two product families

in the carbonyl iron groups; “S” grades and “R” grades. The difference between “S” grades and “R” grades is the purity level; 97.5% in “S” grades and 99.5% in “R” grades [10]. Since the uniform particles distribution and high purity are essential factors for the material synthesis, carbonyl iron powders (CIP) with “R” grades (R-1470) were used in the tests.

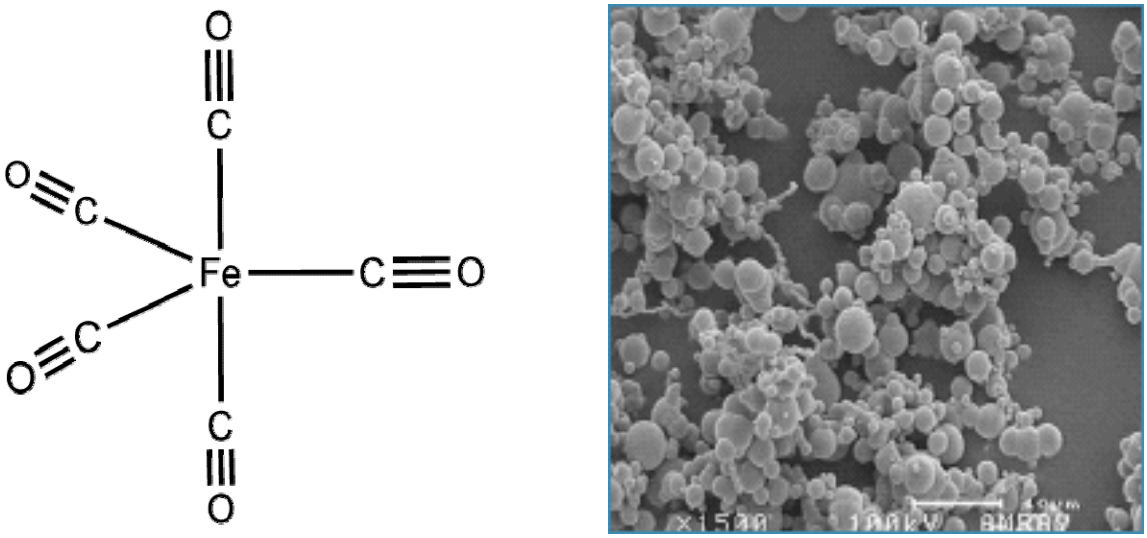

Figure 20.The Structure of Carbonyl Iron Powder. (a) The molecular structure of $Fe(CO)_5$, (b) SEM image of carbonyl iron particles with 97.5% purity (X3500) [10].

In examining biocompatibility, carbonyl iron powders (CIP) show high safety and less toxicity in human bodies. According to the statistical data of the American Association of Poison Control Centers' Toxic Exposure Surveillance System (AAPCC TESS), it is shown that CIP have fewer and less severe symptoms of toxicity as described in Table 4 [10]. The database also shows that the effects CIP is more stable and safer than ibuprofen, which is commonly considered as over-the-counter (OTC) drugs. By the fact, it is possible that CIP can be used in the field of medical applications by their high biocompatibility.

Table 4. Statistics of incidences by the types of medicines overdosed [10].

	Iron Salts (1995)	Iron Salts (1996)	Ibuprofen (1995)	Ibuprofen (1996)	CIP (1995)	CIP (1996)
Moderate Effect	155	117	17	29	1	1
Major Effect	14	5	1	2	0	0
Death	2	2	0	0	0	0
Total	171	124	18	31	1	1
Reported Exposures	21,643	22,382	18,333	21,970	1527	1252
≥Moderate Effect	0.79%	0.55%	0.10%	0.14%	0.06%	0.08

3.1.3. Sodium Tetra-borate ($Na_2B_4O_7 \cdot 10(H_2O)$).

Sodium Tetraborate decahydrate powder, which is sold as "Borax", was adopted as chemical crosslinker for sample synthesis. Its ease of synthesis with PVA and its low cost were the reasons why sodium tetraborate powder was selected as the chemical crosslinker in this work. As shown in the molecular structure of Sodium Tetraborate in Figure 21, when mixed with PVA, the borate ions from the Sodium Tetraborate bond with four oxygen atoms in the PVA thus serving to crosslink the PVA. However, even though borax has no hazards associated with the PVA, it is reported that common sodium borate is toxic by ingestion. This fact is an important factor when the synthesized sample is used in the field of medical applications and will require careful rinsing of the crosslinked PVA to remove any unused sodium tetraborate.

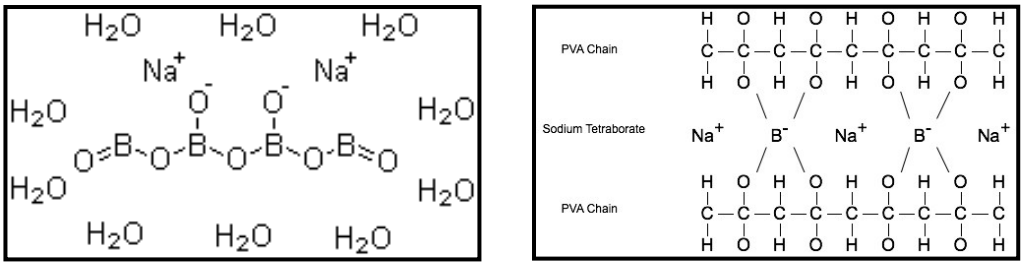

Figure 21. The Strructure of Sodium Tetra-borate.
(a) The molecular structure of Sodium Tetraborate [6],
(b) Schematic of a chemically crosslinked PVA gel [21].

3.2. Samples Preparation Methods.

PVA can easily be gelated to include iron powders using crosslinking methods while it is produced. In general, crosslinking methods are classified as two types of the methods; physical and chemical crosslinking.

3.2.1. Physical Crosslinking.

The physical crosslinking method subjects the polymer to a series of Freeze-Thaw Cycles (FTC). Introduced by Peppas in 1975, a PVA gel or PVA hydrogel can be obtained by Freeze-Thaw Cycles (FTC) which are one of the crosslinking methods. In Peppas' work, aqueous solutions of between 2.5 and 15 wt% PVA were frozen at -20$^{\circ}C$ [70]. The temperature is considered as a freezing temperature. Next, "the samples thawed back to room temperature which results in the formation of crystallites." [70] During the freeze-thaw cycles, cross-linking phenomena occur in the structure of a PVA gel as shown in Figure 22.

By several mechanisms, it is said that the hydrogen bonding described above plays an important role in cross-linking. Chu says that "molecular hydrogen bonding between hydroxyl groups can provide some cross-linking." [71] Plus, Chu described that there are crystal nuclei obtained by freezing and their sites grow into crystal by thawing [71]. Finally, such crystals act as cross-linking sites in the polymers such as PVA gels. Hassan also said that "the thawing process allows the molecules to realign and hydrogen bond to form crystallites. Larger and more numerous crystallite sites form to produce a rubber-like gel." [71] There have been a lot of studies which deal with freezing time, thawing time, PVA concentration, and numbers of FTC which all affect the characteristics of PVA gels prepared using FTC.

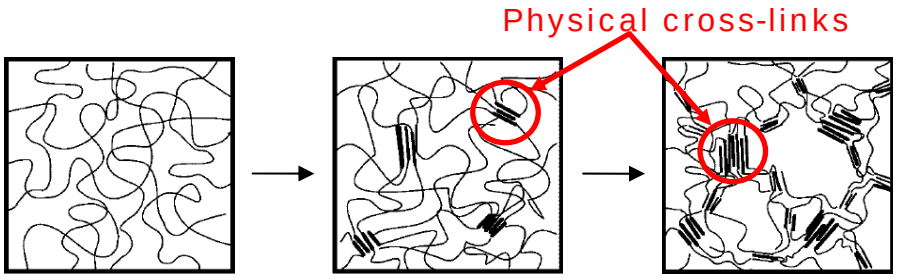

Figure 22. Schematic of physical crosslinking.
(a) Fresh Solution, (b) FTC=1, (c) FTC=3 cycled / aged.

A lot of papers show that the freezing temperature varies from -50°C to close to zero. Mori put the freezing temperature at -50°C using three freezing and thawing cycles in the study [72]. In this paper, Mori described that "The solution was obtained by dissolving 7.5 g of PVA in 80 g of water, this was frozen at -50°C for 3 hours and then warmed up to room temperature over 10 hours [72]." This freezing-thawing process was repeated once again and a hydrogel was obtained. Next, Mori analyzed its tensile strength and elongation [72]. It is said that its tensile strength was 0.6MPa and the elongation at break was 130% [72].

Table 5. The optimized freeze-thaw cycle (FTC). (1 cycle)

- Cooled with 0.5°C/min to −20°C.
- Kept at the freezing temperature for 6 hours.
- Thawed with 0.3°C/min to 25°C.
- Kept at the thawing temperature for 3 hours.

Based on the papers by Chu, Hassan, and Mori, it was decided that at least three freezing and thawing cycles should be adopted for samples to behave properly. Since one cycle takes about 20 hours in the paper by Chu [71], it is time-consuming if there are more cycles than three cycles. However, even though three cycles was selected to reduce production time, it still takes about 60 hours to produce samples. To reduce time for sample preparation, changes of freezing and thawing time were conducted and the optimized time was set up for one cycle as shown in Table 5.

The optimized production time was set up as about 11 hours for one cycle. As shown in Figure 23 (a), a temperature chamber was used to keep exact temperature conditions based on the FTC method. After three cycles, which take about 33 hours, ferrgogel samples were prepared as shown in Figure 23 (b). The example is a sample made of 12wt. of PVA and 5wt. % of CIP. Changing amounts of PVA and CIP, nine ferrogel samples with physical crosslinking method could be obtained for this study; there are three different weight percentages of PVA and CIP.

(a) (b)

Figure 23. Physical Crosslinking Method.
(a) A Temperature Chamber used for FTC [Model115, TESTEQUITY].
(b) Ferrogel samples.

When ferrogel samples are obtained from the three optimized cycles, all of the samples had been dehydrated during the thawing process, whose temperature is $25^{\circ}C$, as shown in Figure 24. This phenomenon is common when all of hydrogels without any treatments are produced because water in each sample is exposed to air during any process. Thomas described that all of hydrogels reached 70.4%(1.5h), 46.3%(3h), 25.1%(7.75h), and 10.3% (24h) of their initial masses when they were kept in a vacuum oven at $37^{\circ}C$ [73]. The same was true for ferrogel samples in this study. Since the dehydration causes errors and changes of percentage of PVA and CIP, a rehydration process is required in ferrogel preparation. The samples were rehydrated by soaking each dehydrated sample into the shaping mould at room temperature and returning its volume to the original value. After about four hours, ferrogel samples were re-prepared.

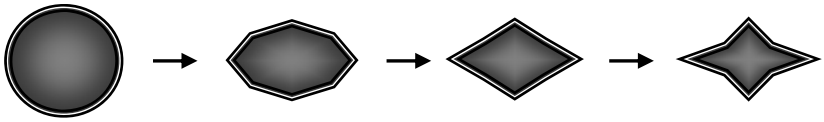

Figure 24. Schematic of the changes in cylindrical sample shape with dehydration (side view).

3.2.2. Chemical Crosslinking.

In this method, samples were produced by chemically cross-linking poly(vinyl) alcohol (PVA) using sodium tetraborate. As mentioned above, sodium tetraborate serves to crosslink chains of PVA by binding oxygen ions in PVA with the borate ion of sodium tetraborate as shown in Figure 21. First, samples were produced by mixing the PVA powder and sodium tetraborate powder and then adding the appropriate amount of distilled water. 1:1 ratios of PVA and sodium tetraborate were used in order to ensure that full crosslinking was accomplished. Next, when the powders were completely dissolved in the water, iron powder ($Fe(CO)_5$ from ISP Technologies, Inc.) was mixed into the solution. The solution was continuously stirred until it was fully dissolved and a gel was formed. The time for the entire process ranged from five to thirty minutes and more time was needed for the less concentrated solutions.

When it comes to dehydration of samples, there was no exception for chemical crosslinking. It is also because the water content of these gels was exposed to air and thus evaporated at room temperature during the production process. Like rehydration in physical crosslinking, chemically crosslinked samples were placed in distilled water and re-hydrated to their original consistency. Another observation was that these samples are easily contaminated by dirt and dust in the environment.

Many of these observations suggest the improvement for enclosing these samples in a sealed membrane if they are to be used in applications.

3.3. How a Ferrogel Works.

When it comes to the ferrogel behaviors, it is important to understand the principle of the common magnetic particles and bulk strains. When a magnetic field is applied, magnetic particles in synthesized samples are magnetized and aligned through the direction of a magnetic field applied. To understand bulk strains of ferrogels, it should be assumed that ferrogel behaviors follow the conservation of the volume despite their contraction due to the magnetic field.

3.3.1. The Principle of the Magnetic Particles.

The Figure 25 shows that the magnetic particles are aligned through the magnetic field direction when the magnetic field is applied. When there is no external magnetic field, CIP is randomly and uniformly distributed in the sample after sample synthesis as shown in Figure 25 (a). Then, when an external magnetic flied is applied near the magnetic particles, the magnetic field results in the magnetization of particles. Magnetization is defined that a particle has a tendency to have its own polarity by the magnetic field direction. As a result, particles of CIP in synthesized sample are aligned through particle lines as shown in Figure 25 (b).

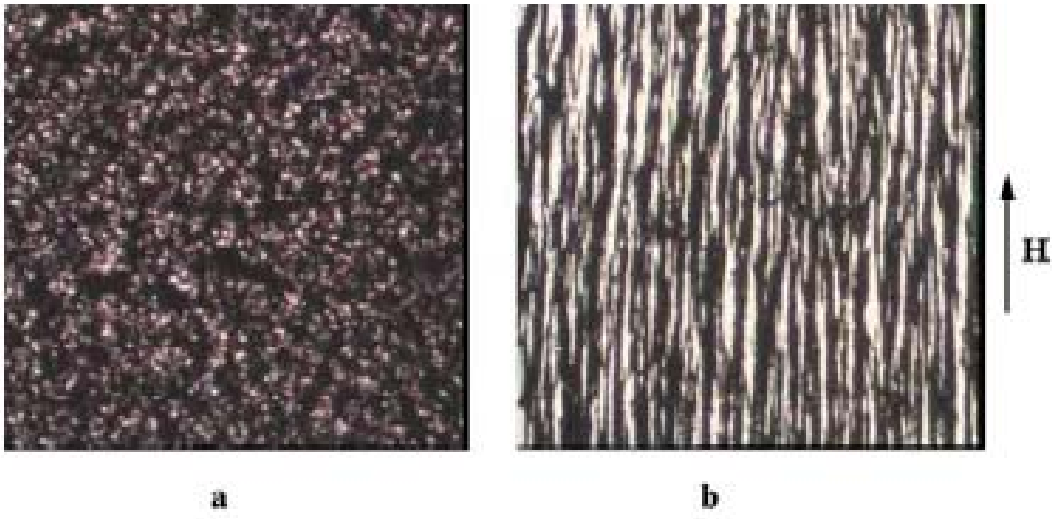

Figure 25. Formation of magnetic particles in silicon oil (5 wt%) [15].
(a) No external magnetic field. (b) The magnetic induction 50 mT.

3.3.2. The Principle of Behaviors of Ferrogels.

In this thesis, data is presented for an inhomogeneous field applied along the axis of ferrogel samples using permanent magnets. The bulk strain mechanism for these tests was occurred with both physical and chemical crosslinking methods and is sketched in Figure 26. The magnetization of the magnetic particles which occurred in the gel matrix is initially random as shown in Figure 26 (a). Next, Figure 26 (b) shows that when the sample is brought close to end of the permanent magnet, the magnetic particles align with the field and move towards the highest magnetic field (ie: the surface of the magnet). Because the matrix material is highly flexible, the matrix moves with the magnetic particles causing bulk strain. The magnetic attraction is counteracted by the internal friction of the viscoelastic matrix as well as the weight of the sample itself.

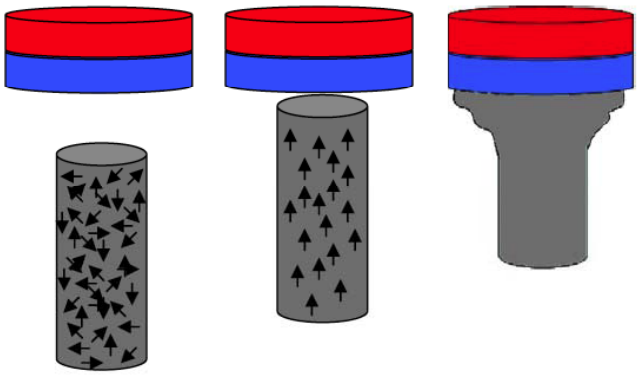

Figure 26. Ferrogel behavior when exposed to a permanent magnet.

Chapter 4. EXPERIMENTAL SET-UPS

The objective of this study is to characterize the actuator behavior of the ferrogels synthesized using physical and chemical crosslinking and a variety of amounts of PVA and CIP as described above. Interests in this study are the measurements of the free-strain and the loaded behavior of the ferrogels.

The basic testing apparatus used is described in Figure 27 and Figure 28. The ferrogel samples were shaped into 20 mm long cylinders with a 4 mm diameter. Initially, these samples were suspended vertically from a single permanent magnet (H=0.2T). The sample was placed within a semi-cylindrical straw in order to ensure vertical contraction and reduce the effects on any bending of the sample caused by its non-uniformity. To reduce the effect of friction between the sample and the straw, the inside surface of the straw was lubricated. Next, when exposed to the non-uniform magnetic field the sample contracted as shown in Figure 26. This strain was found to be so large that it is enough to be measured with a standard ruler. The behavior of the sample under the field was recorded using a digital (Canon Power Shot TX1 7.1 MP) camera and the strain and strain rate were determined through later processing.

4.1. Tests Apparatuses.

- **Free Strain Tests.**

Based on the set-up described in Figure 27, the free strain test was tested and strains were measured by the ruler and the digital camera. The magnetic field was increased up to 0.25 T by adding up to 4 additional magnets as shown in Figure 28. Since each magnet attracts strongly each other, adding each magnet on another required carefulness not to cause errors due to moving samples.

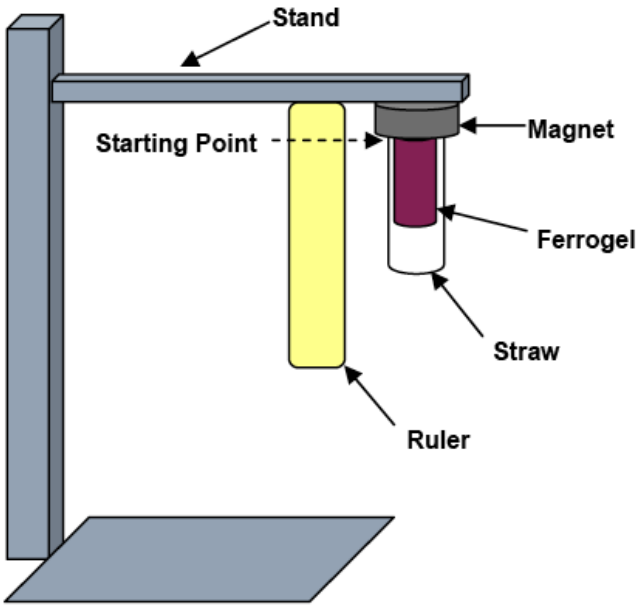

Figure 27. Testing apparatus for free strain.

- **Loading Tests.**

In case of loading tests, a copper wire served as a weighting material because the amounts of loads can be controlled with the length of copper wires. Moreover, it is well-known that copper does not influence the results from magnetic fields because it is a non-magnetic material. The copper wire was threaded through the ferrogel at

the end. It was observed that the ferrogel was not torn due to larger loads. For the loaded cases, copper wires of the appropriate mass from 0.5g to 2g were attached through the base of the gel and were then lifted when the gel was exposed to the field.

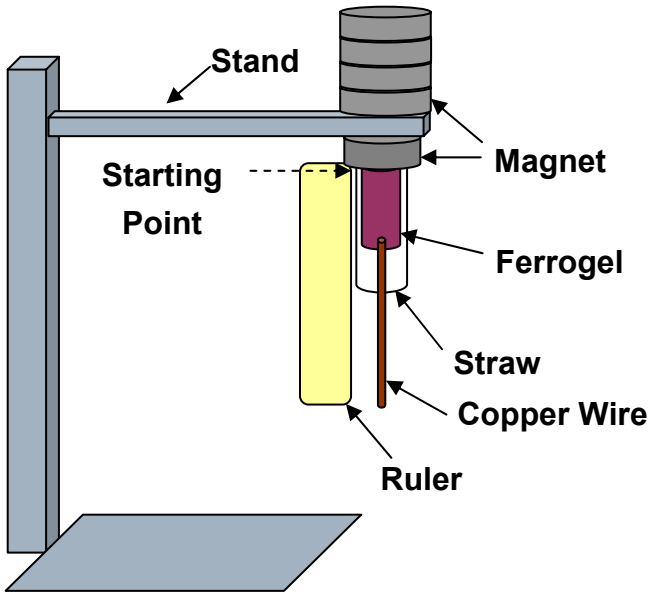

Figure 28. Testing apparatus for loaded tests.

- **Strain Rate Tests.**

These tests were attempted based on the set-up with five permanent magnets (0.25T) as shown in Figure 28, but not loaded. The strain rates were measured under the exactly same condition with amounts of PVA (4 wt. %) and CIP (10wt. %) to compare between two different crosslinking methods. The limit time for measurements was fixed to 25 seconds. Since this test requires the accuracy with the real time, recording with a digital camera was helpful in measuring strain rates.

4.2. Test Matrix

The experimental data presented in the following section is based on a series of tests on a total of 14 samples. The composition of these samples varying with weight percents of PVA and CIP is summarized in Table 6. Samples were synthesized using both physical and chemical crosslinking methods. When it comes to the ratios of PVA and CIP, Table 6 shows that ferrogel samples were synthesized with PVA weight percentages of 4, 8, and 12 and iron weight percentages of 1, 5, and 10.

Table 6. Samples synthesized for this study.

Physical Crosslinking					Chemical Crosslinking				
PVA (wt.%)	CIP (wt.%)				PVA (wt.%)	CIP (wt.%)			
		1%	5%	10%			1%	5%	10%
	4%	x	x	x		4%	x	x	x
	8%	x	x	x		8%			x
	12%	x	x	x		12%			x

Each of the samples was tested for both free strain and strain under load. The five permanent magnets were used to expose the samples to magnetic fields ranging from 0.2 T to 0.25 T. Even though the magnetic field was applied along the axis of the sample, there was the concentrated magnetic field at the end of the sample closest to the magnet as shown in Figure 29. It is expected that there is a relationship between magnetic field and vertical distance from the end of a magnet. This relationship can be obtained by using an AC/DC magneto-meter (AlphaLab,Inc.) and an axial probe.

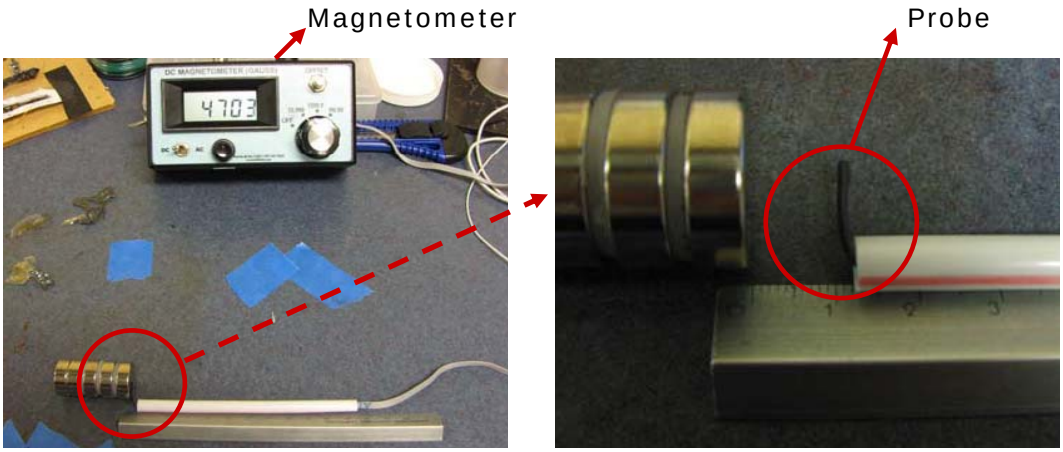

Figure 29. Measurement of magnetic field gradients as a function of distances.

As described in Figure 29, since it is unstable to keep the flexible wire straight, a plastic straw was used for the probe to be straightened vertically with the direction of a magnetic field. Figure 30 shows the magnetic field gradient.

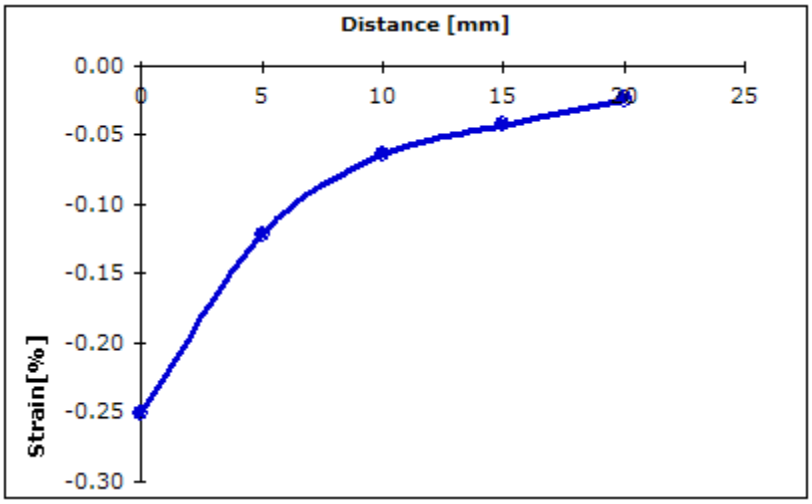

Figure 30: Magnetic field distribution in the sample

As Figure 30 shows the magnetic field gradient is a function of distance, the strength of magnetic field at the end of five magnets attached together recorded about

-2500 Gauss, which is calculated as 0.25 T. From the end to a distance of 5mm, the field gradient has shown a very steep slope of the curved line, which is sensitive to a distance. Compared with this slope of the line, there is no difference between a distance of 10mm and 20mm. It is expected that similar trends occur for any number of permanent magnets. Such a measurement of the field gradient is necessary to explain and predict the actuator behaviors of ferrogels. It is also important to note that this axial field is perpendicular to the magnetic fields applied by electromagnets in the literature [74]. Moreover, it is reasonable to use samples with a length of 20mm as mentioned above in this research.

Chapter 5. RESULTS AND DISCUSSION

5.1. Free Strain Tests.

For these tests, samples of various PVA and CIP compositions as well as samples synthesized using chemical and physical crosslinking are hung from the apparatus discussed in Chapter 4. The strain induced by the magnetic field was measured as the field is increased by adding permanent magnets to the apparatus. The results for the physically crosslinked samples are shown in Figure 31.

As can be seen, both the PVA weight percent and the CIP content influence the amount of strains. It is generally known that as the PVA weight percentage is increased, there are more PVA chains to be crosslinked during the freeze-thaw cycles. For that reason, the matrix material with more PVA shows higher stiffness. Therefore, as an inhomogeneous magnetic field is applied to the ferrogel, the magnetized particles cause a contraction of the bulk sample. During its contraction, less strain of the sample with more PVA will occur. This hypothesis is verified by the data in Figure 31 which is summarized in Table 7 (a).

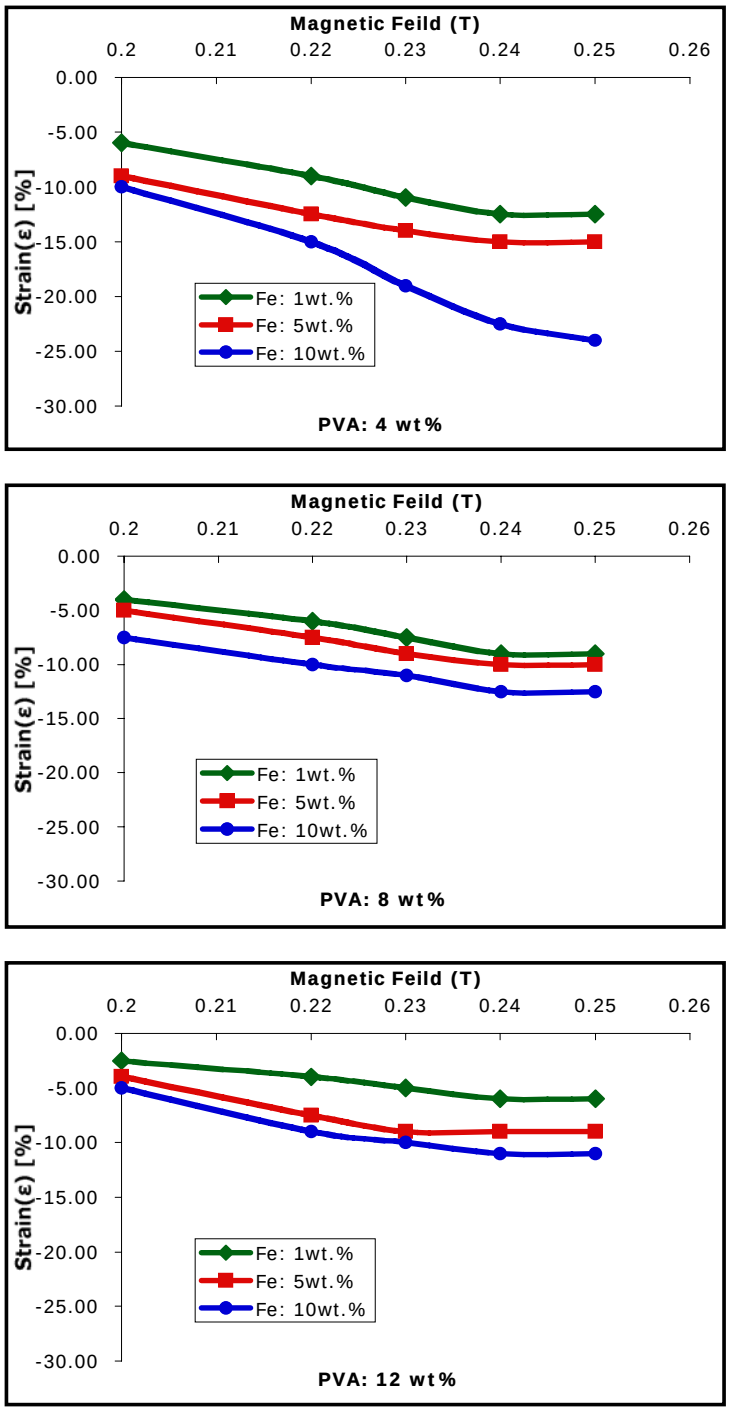

(a) PVA: 4 wt%
CIP: 1,5,10 wt%,

(b) PVA: 8 wt%
CIP: 1,5,10 wt%,

(c) PVA: 12 wt%
CIP: 1,5,10 wt%.

Figure 31. Free strain under field for selected PVA and CIP weight percents.

The weight percent of iron added in the ferrogel also plays an important role in determining the maximum free strain of the ferrogels. The free strain is due to the attraction of the iron particles to the areas of larger magnetic field. As the particles move towards the largest field, the matrix deforms and produces a bulk strain. Thus, as more iron is embedded it is expected that larger strains will be accomplished. This is verified by the data collected shown in Figure 31 and Table 7 (a). However, it is important to note that there is an upper limit to the amount of iron that can be embedded in the ferrogel because the ferrogel is also governed by the ability of the PVA chains to form physical bounds to the iron particles.

Free strain was also measured for the chemically crosslinked samples. These samples had lower moduli than those of physically crosslinked samples. It implies that it needs to be shaped into the cylinders of the appropriate size. Moreover, these samples also dried out during the tests and had to be exchanged with other samples. These considerations for chemically crosslinked samples led to more variation in the tests results seen in Figure 32.

There are several important observations from the data seen in Figure 32. First, the chemically crosslinked sample with 1 wt% iron can be considered. When low field levels are applied, the strain in this sample is positive corresponding to the situation in which the weight of the sample causes it to stretch. It implies that the effect of magnetic field applies was not able to overcome its gravitational effect. At high enough fields, the weight of the sample is balanced by the magnetic force on the particles and thus the sample does not strain. These results indicate that the iron particles in these gels improve the mechanical strength of the samples as well as provide the mechanism for strain in a magnetic field. Thus, those samples with more iron content stretch less under their own weight.

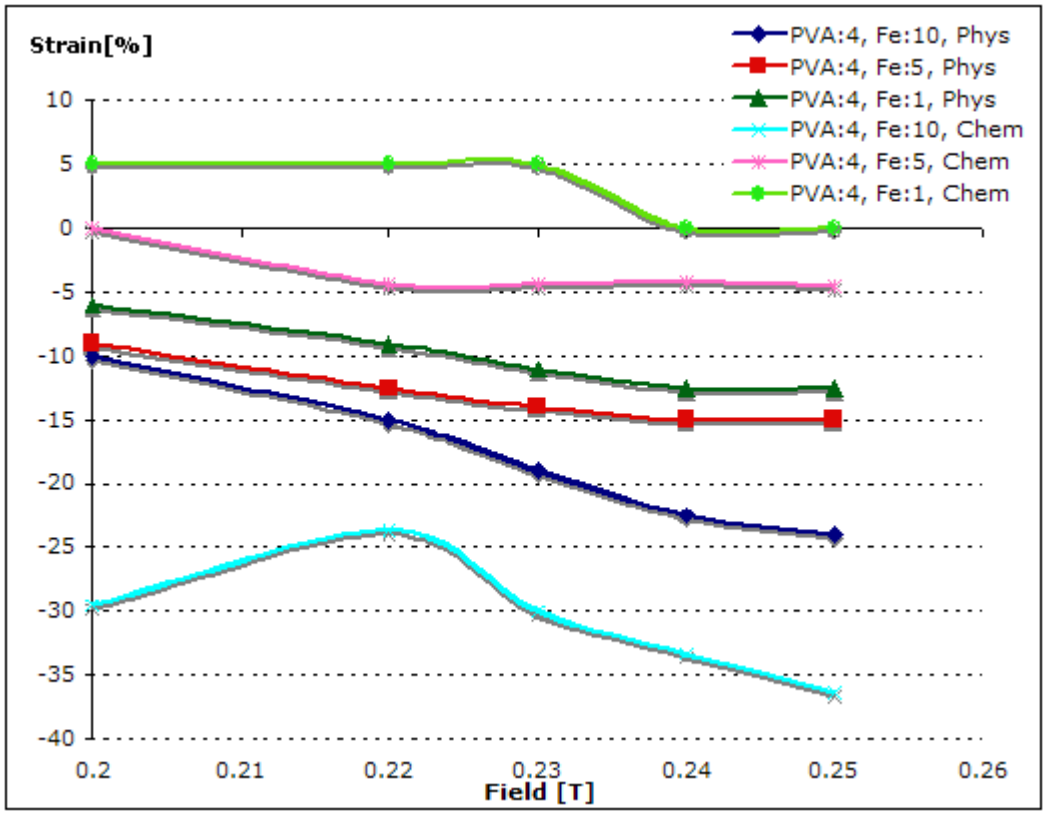

Figure 32. Free strain for PVA: 4% and various iron content for both physical and chemical crosslinking.

As shown in Figure 32, the chemically crosslinked samples with 5 wt% CIP exhibit saturation at low fields. When two magnets (H = 0.22T) are applied, all of the CIP content has reacted to the magnetic field and increase of the permanent magnets in field has no effect on the strain of the sample. A similar effect is seen in the physically crosslinked samples with 1 and 5 wt% CIP.

The largest strains are achieved from the chemically crosslinked sample with 4 wt% PVA and 10 wt% iron. This sample is also the most flexible among the samples and it shows the highest rate of dehydration when exposed to air. This explains why the first test on this sample achieves larger strains while it is still moist than does the second test once it has dried. The strain then increases steadily

reaching a maximum of 36% and has not saturated when the maximum of the magnetic is applied. This indicates that further increase in field levels will allows the sample to achieve larger strains. This will be the subject of further tests in which the issue of the samples drying when exposed to air will also be addressed.

Table 7: Free strains at largest field (.25 T) for all tested samples.

(a) Physical Crosslinking.

Physical Crosslinking				
PVA (wt.%)	CIP (wt.%)			
		1%	5%	10%
	4%	-12.5	-15	-24
	8%	-9	-10	-12.5
	12%	-6	-9	-11

(b) Chemical Crosslinking.

Chemical Crosslinking				
PVA (wt.%)	CIP (wt.%)			
		1%	5%	10%
	4%	0	-4.5	-36
	8%			-7.7
	12%			-2.7

The largest strain measured from each of the samples synthesized is shown in Table 7. The largest strain was seen for the 4 wt% PVA and 10 wt% iron samples for both the physically and chemically crosslinked samples. These samples were the most flexible because they have low PVA chains and the high sensitivity due to their high CIP content. The largest overall strain was found for the chemically crosslinked sample because it had a lower stiffness than the physically crosslinked one. The higher PVA content chemically crosslinked gels were difficult to produce because they are stiffened quickly as the PVA content was increased and thus were not prepared.

The largest measured strain was 36% in the maximum of the field, 0.25 T. This compares very favorably with smart materials as well as being consistent with other ferrogel tests reported in the literature [28]. Among materials categorized as “smart materials”, Electro-Active Polymers (EAPs) are most known for their large strains.

Compared with EAPs, most of these strains show about 10% even though strains of up to 200% have been measured for dielectric EAPs by the literature [27]. Thus, the measure of 36% strain with ferrogel samples and the possibility for more in larger fields suggests applications for these materials in the future. A comparison of strain levels with similar ferrogels prepared by Zrinyi et al. shows similar trends in PVA and CIP percentages. The strain level in the literature is measured up to 40% of the strain even though the field levels in that case were 3 times as large.

5.2. Loading Tests.

The loaded tests were run on the samples with 4 wt% PVA and 10 wt% CIP which exhibited the largest free strains. The testing apparatus was same as that of free strain tests except that weights of up to 2 grams were attached to the bottom of the samples. Then, the samples were exposed to 0.25 T fields and their strain under load was measured. These results are shown in Figure 33 for both the chemically and physically crosslinked samples.

There is a distinct difference between the behavior of the softer chemically crosslinked samples. The fact shows that the physically crosslinked sample have higher stiffness. Though the chemically crosslinked samples begin with the larger free strain as soon as a load is added, this strain is stretched sensitively to increase of loads. When the load is increased to about 1.7 grams the sample is unable to strain and the blocked load has been reached. Above 1.7 grams, the sample shows an elongation of the sample due to the added load.

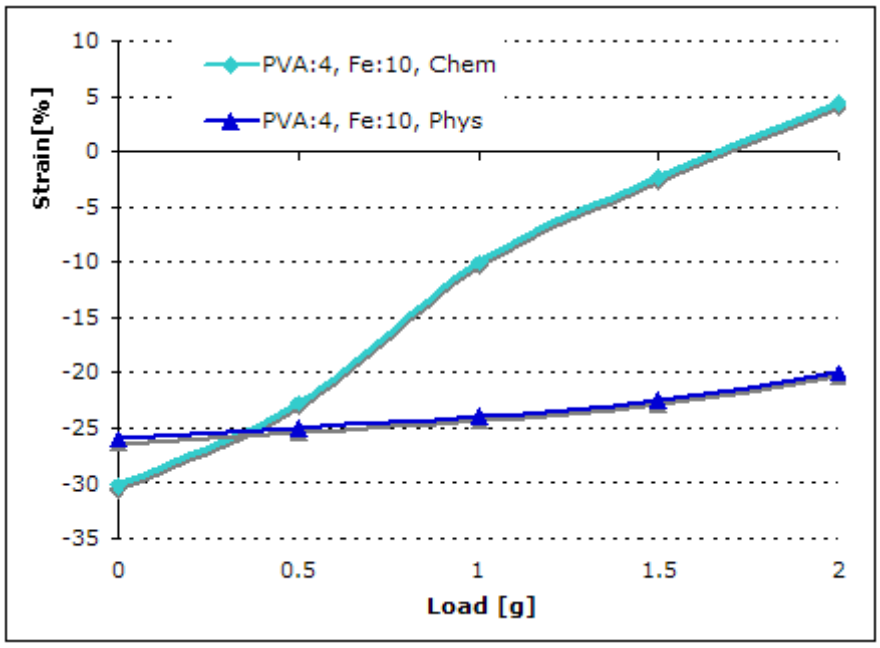

Figure 33. Strain achieved under loads for field levels of 0.25 T.

On the other hand, the physically crosslinked sample does not show a considerable decrease in strain as it is loaded up to 2 grams. As shown in Figure 33, the strain only decreases by about 20% under the load of 2 grams. According to the trend established in Figure 33, it is possible to predict more strains due to larger loads in future tests. It is important to note that though 2 grams (20 mN) are not a large or useful loading level; these samples only weigh about 0.5 grams. The fact means that they can lift 400% of their own weight. To compare with other materials and ferrogel samples considering sizes of materials, it is reasonable to calculate the energy density of these materials.

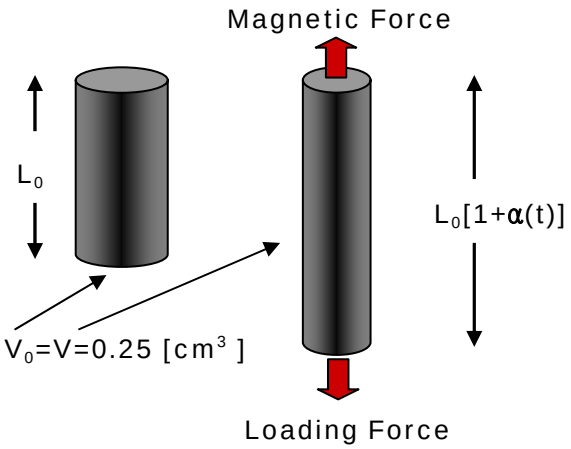

Figure 34. Schematic of the ferrogel behavior under the loading tests.

Since the loading tests assume that the volume of ferrogel is constant and the ferrogel behaviors are not dependent upon time, the following is the changes of sample volume and length.

$$V_0=V=0.25\ [cm^3],$$

$$L_0[1+\alpha(t)] = L_0(1+\alpha) = L_0(1.2) = 24\ [mm]$$

To get a value of work done by the sample,

$$[\text{Work done}] = [\text{Loading Force}] \cdot [\text{Displacement}]$$

$$= (20)\ [mN] \cdot (24\text{-}20)\ [mm]$$

$$= 80\times10^{-6}\ [J]$$

Then, the energy density (defined as energy per unit volume) is,

$$[\text{Energy Density}] = \frac{[Energy]}{[Volume]}$$

$$= \frac{80\times10^{-6}}{0.25\times10^{-6}} \quad \frac{[J]}{[m^3]} = 320 \quad [J/m^3]$$

The work performed by the physically crosslinked sample is 80×10^{-6} [J], while its volume is 0.25 cm^3 as shown in Figure 34 above. As described above, the energy density is calculated as 320 J/m^3. The value is comparable to the energy density of 400 J/m^3 that was achieved by Zrinyi et al. [13] in fields 3 times as large. Of course, it is promising as compared with other smart materials.

5.3. Strain Rate Tests.

Lastly, the set of data collected was a study of the strain rate in the samples. These tests were also run for the samples which showed the most strain; that is the 4 wt% PVA and 10 wt% CIP samples. The results are shown in Figure 35 which shows that the behavior of the physically and chemically crosslinked samples vary considerably. The physically crosslinked samples were tested for both the smallest and largest field levels (0.2 and 0.25 T). As can be seen, these samples strain abruptly as soon as they are closest to the magnets. Then, they hold a steady strain for the remainder of the tests for about five seconds and were saturated above five seconds. However, the chemically crosslinked sample strains suddenly when first exposed to the field but continues to increase that strain until the test ends. This behavior can be explained that the chemically crosslinked samples have lower stiffness.

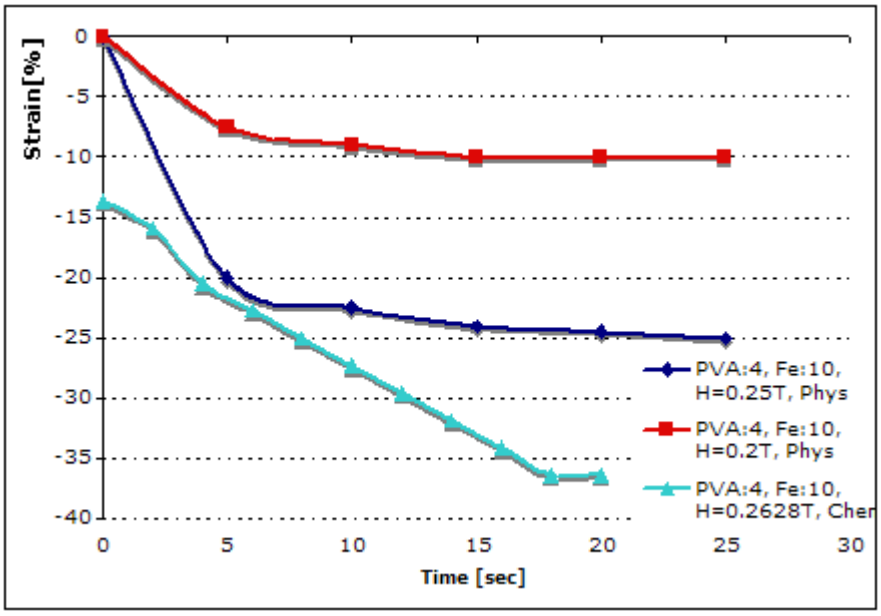

Figure 35: Strain over time for physically and chemically crosslinked samples.

5.4. Summary

The primary focus of this thesis was on the comparison between chemically and physically crosslinked samples. Plus, the conclusions of this thesis were also based on the effect of PVA and CIP concentrations. These conclusions are summarized in the bullet points below:

- The *synthesis method for the chemically crosslinked samples is much easier* because it requires a most 30 min as opposed to about 33 hours for the physically crosslinked synthesis. However, physical crosslinking does not require the use of any external crosslinking chemical and thus results in complete biocompatibility.

- The chemically crosslinked samples which were prepared have considerably lower modulus and more dominated by viscosity than the physically crosslinked samples with the same amounts of PVA and CIP.

- For both chemically and physically crosslinked samples, it was found that the *4 wt% PVA and 10 wt% CIP ferrogels exhibited the largest strains* in a given magnetic field. This sample composition represented the fact that the lowest modulus samples tested with the most magnetic particles allow the field to have a greater effect on the strain. However, previous testing with the chemically crosslinked samples has discovered that there is a lower limit to the amount of PVA for samples to maintain their structural integrity.

- The free strain testing showed that the largest strain produced under 0.25 T fields was 36% and was achieved by the chemically crosslinked sample, while they physically crosslinked one achieved maximum free strains of 24%. This was expected since this sample has lower stiffness than that of the physically crosslinked sample and thus had less resistance to motion. This observation implies that if *large free strains* are required, *chemical crosslinking* should be considered.

- In the strain under load tests, the physically crosslinked sample showed less than 20% drop in strain achieved when loaded up to 2 grams (equal to 400% of its weight) and such a 20% drop in strain corresponds to an energy density of 320 J/m^3. The chemically crosslinked samples exhibit a dramatic decrease in maximum strain as they are loaded and above about 1.7 g they reach their blocked load and are unable to

strain under the maximum field. Thus, if the design constraint requires *high loading capability*, then *physically crossslinking* should be considered.

- The results of the rate tests also shows a distinct difference between chemically and physically crosslinked samples. The chemically crosslinked samples strain suddenly when first exposed to the magnetic field and then continue to strain at a linear rate throughout the 20 second test. The physically crosslinked samples strain to their maximum strain in the first 5 seconds of the tests and do not exhibit further strain during other 15 second test.

- Table 6 shows the characteristics of ferrogels synthesis on different crosslinking method. It was summarized based on this research results described above.

Table 8. Characteristics Comparison between Physical and Chemical Crosslinking.

Physical Crossliking	Chemical Crosslinking
1. Larger Loaded Strains. **2. Longer time to synthesize and produce. (33 hours)** **3. Stiffer and better retain their original shape.**	**1. The capability for larger free strains.** **2. A fast synthesis time (5-30 mins).** **3. Highly flexible and take the shape of their container.**

Chapter 6. CONCLUSION AND FUTURE WORK

6.1 Conclusion

This thesis has presented the experimental results for the free strain and loaded behavior of 14 ferrogel samples as well as the introduction of ferrogels. This thesis shows the classification of the smart materials to help understand ferrogels. A ferrogel, a topic in this thesis, has been one of low modulus smart magnetic materials. A ferrogel can be considered as a new class of magneto-controlled elastic materials and are synthesized with crosslinking between polymer chains and magnetic particles. Table 3 shows researches on ferrogels and their summaries were mentioned in this thesis. Likewise, each type of the smart materials were introduced and some free strains were compared with that of ferrogels as shown Table 9.

Table 9. Comparison of free strains in smart materials.

Type		Free strain	Example
PZT		0.1% [9]	SiO_2
SMAs		-	Ni-Ti alloys
EAPs		10% [19]	Electric / Ionic
Magnetic Materials			
High Modulus	Magnetostrictive	1% [44] [45]	Terfenol-D / Galfenol
	FSMA	10% [5]	Ni-Mn-Ga alloys
	Others	Magnetoresitive and Magnetocaloric	
Low Modulus	MR Fluids	-	-
	MREs	0.1% [20]	Dampers
	Ferrogel	40% [31]	PVA / Gelatin Gel

Such a behavior of ferrogels was enough to motivate for characterization. For sample preparation, gelatin was first selected but PVA was done as the main material because gelatin was easily contaminated within 24 hours. Plus, Carbon Iron Powder (CIP) was selected as magnetic particles because of its high biocompatibility and purity as well as the uniform particles distribution. For chemical crosslinking, sodium tetraborate was used as a crosslinker because of its ease of synthesis with PVA and its low cost.

Next, the two crosslinking methods were used: standard chemical crosslinking using sodium tetraborate and physical crosslinking using a series of freeze-thaw cycles optimized to reduce production time. In addition, the amounts of PVA and iron power used for the samples were varied in order to establish trend dependencies of various factors. Key findings is that the chemically crosslinked samples can strain up to almost 40% and the physically crosslinked samples can strain within 20% of the maximum strain even when loaded to 4 times their own weight. The experimental data indicate that the behavior of ferrogels is highly dependent on amounts of PVA and CIP as well as the crosslinking method used. In summary, while standard chemical crosslinking methods are easily and quickly completed (30 minutes) and samples show large strain capabilities, the physical crosslinking methods result in stronger samples with the ability to strain under larger loads and are completely biocompatible. It means that the choice of crosslinking method as well as composition for ferrogels should be based on the specific desired application.

6.2 Future Work.

The work presented in this thesis represents a preliminary study done with experiments for future works to be done. The results show promise for larger strains if larger fields are applied. In addition, the physically crosslinked samples did not achieve their blocked force under the loads applied in this work. The work indicated that the softer samples were the most active in all cases, however, it is predicted that there is some lower limit to the amount of PVA required and thus there is still optimization of PVA, crosslinking density, and iron compositions that needs to be studied. Finally, all of this experimental data will be form the basis for predictive modeling that will provide a more thorough understanding of the materials behavior as well as the ability to specifically design a material for a given application.

- **Reversibility & Repeatability.**

In this study, all of samples have some limitations for their reversibility and repeatability. If measurement processes can be reversed and repeated on the same set of inputs, the function or process can be reversible [75]. In the case of repeatability, it is defined as the property that the independent results obtained with the same conditions after intervals of time have no difference [75]. In this study, the reversibility and the repeatability of ferrogels have been not considered and tested. However, it is known that the dehydration of ferrogels interrupt those properties. Such dehydration results in change of the ferrogel stiffness and thus most of samples could not reverse to their original shape. Above all, the dehydration problems should be solved to improve the two properties. If the yielding strength of a ferrogel is measured keeping the content of water in the ferrogel, it can have its reversibility

and repeatability under its elastic deformation. To increase the reversibility and repeatability, it is needed to enclose samples in a sealed membrane or coated film to avoid dehydration.

- **Larger Magnetic Fields and Loads.**

Under loading tests mentioned above, ferrogel samples with a physical crosslinking method showed a higher loading capability than 2 grams tested. As shown in Figure 33, the gentle slope of the curved line with physical crosslinking implies that it is possible for the physical crosslinked ferrogel to endure more loads than 2 grams. It is also important factor that it could be torn due to concentrated load at the contact with the wire before the maximum is measured. It is important to identify the maximum load possible so that the usefulness of these materials in various applications can be determined. The free strain tests showed that the chemically crosslinked samples had not reached saturation of the highest magnetic field in this study. Considering the maximum strain of about 40% under 840 mT measured by Ramanujan [31], it is possible to achieve maximum strains more than 36% under larger magnetic fields.

- **Mathematical Modeling.**

This research shows that ferrogel behaviors have large strains up to 36% and their stress-strain curve would be non-linear deformation. Those facts imply that ferrogel behaviors have hyper-elasticity. Plus, since the samples are controlled by a magnetic field applied, the strength of the magnetic field, H, should be in the mathematical modeling. If strains in hyper-elasticity are considered on measurements, the independent variables would be as following.

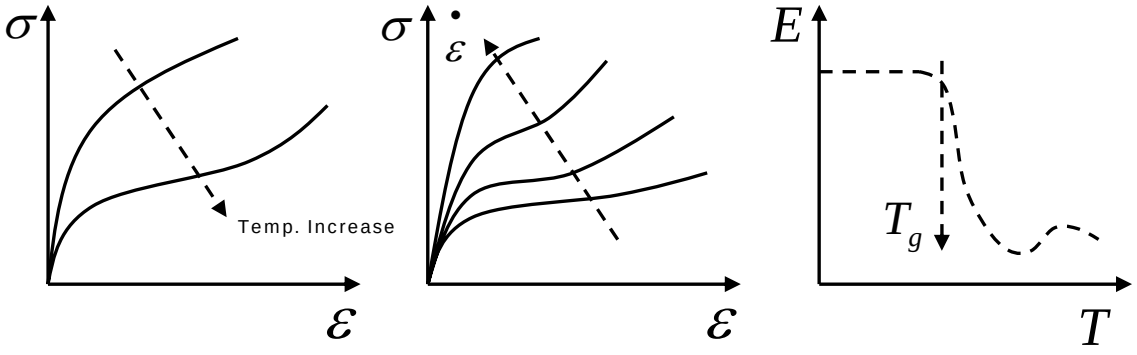

$$\varepsilon = \varepsilon(H, T, \dot{\varepsilon}, \varepsilon_0)$$

when H =Magnetic Field, T =Temperature, ε_0 = History of loading (total strain).

Based on theories related with hyper-elasticity, the mathematical modeling could be analyzed. The modeling on the dynamic deformation of ferrogels enables researches on the ferrogels to be improved and developed.

- **Applications**

Compared with EAPs mentioned above, ferrogels enable the control inputs to be remote system without physical connection. Considering unique advantages of ferrogels, their applications in the future would be diversified. Of course, ferrogels can be substituted for EAP used in the field of biomimetic applications as well as artificial muscles in medical industries. Next, ferrogels can serve as actuators with macro-scale strains in remote systems in a variety of industries. Lastly, owing to high biocompatibility of ferrogels, they promise that it is possible for the ferrogel to be used in biomedical applications such as drug delivery systems.

REFERENCES

1. Jiles, D.C., *Introduction to Magnetism and Magnetic Materials*. 2nd ed. 1998, New York: Chapman, & Hall.
2. Brain, M. *How Airbags Work.* HowStuffWorks.com 2000 14 April 2008 [cited; Available from: http://auto.howstuffworks.com/airbag.htm.
3. CSU, S.C.D., *The Structure and Properties of Polymers*. 2000.
4. Piezomaterials., *The Piezoelectric Effect.*, www.piezomaterials.com/piezoeffect.jpg, Editor. 2007.
5. Hakola, A. *Ferromagnetic Shape-Memory Materials* 2006 [cited 2008 April 25]; Available from: http://www.tkk.fi/Units/AES/projects/prlaser/msm.htm.
6. RSC, *A crossed-linked polymer*. 2005, Royal Society of Chemistry.
7. Bhattacharyya, A., *Smart Materials* 2001, SMA/MEMS Research Group,University of Alberta.
8. Lagoudas, D.C. *Introduction to Shape Memory Alloys*. April 25, 2008 [cited; Available from: http://smart.tamu.edu/overview/overview.html.
9. Novotny, M. and P. Ronkanen. *Piezoelectric Actuators*. April 24, 2008 [cited; 12]. Available from: http://www.ac.tut.fi/aci/courses/ACI-51106/pdf/Piezo/PiezoelectricActuators.pdf.
10. ISP, *Ferronyl Iron*. 2006, International Specialty Products.
11. Socki, J., *A Process-Capable System for Hermetic Solder Sealing of Tight Tolerance Crystals*, in *13th Piezoelectric Devices Conference and Exhibition, Vols 1 and 2*. 1991. p. A64-A69.
12. Wisconsin, U.o., *Nickel-Titanium: A Shape Memory Alloy*. 2002, The Board of Regents of the University of Wisconsin System.
13. Zrínyi, M., *Intelligent polymer gels controlled by magnetic fields.* Colloid & Polymer Science, 2000. **278**(2): p. 98-103.
14. Song, G. and M. Zeng, *A thin-film magnetorheological fluid damper/lock.* Smart Materials & Structures, 2005. **14**(2): p. 369-375.
15. Varga, Z., G. Filipcsei, and M. Zrinyi, *Smart composites with controlled anisotropy.* Polymer, 2005. **46**(18): p. 7779-7787.
16. Daniel Christ, S.R., *Numerical Simulation of the Application of NiTi Alloys in Medical Technologies.* PAMM, 2005. **5**(1): p. 387-388.
17. Ryhänen, J., *Biocompatibility evaluation of nickel-titanium shape memory metal alloy*, in *Faculty of Medicine, University of Oulu*. 1999, University of Oulu: OULU FINLAND
18. Straub, F.K., et al., *Development of a piezoelectric actuator for trailing edge*

flap control of full scale rotor blades. Smart Materials and Structures, 2001. **10**: p. 25-34.

19. Akbay, M.C., *Performance of compliant electrodes in electro active polymer (EAP) actuators*, in *Textile Management and Technology of North Carolina State University*. 2004, North Carolina State University: Raleigh, North Carolina.
20. Guan, X., X. Dong, and J. Ou, *Magnetostrictive effect of magnetorheological elastomer.* Journal of Magnetism and Magnetic Materials, 2008. **320**(3-4): p. 158-163.
21. Park, G., E.J. McLaurin, and L.E. Faidley, *Characterization of the Actuator Behavior of Blended-system Ferrogels.*, in *SPIE*. 2008: San Diego, California.
22. Dapino, M.J., R.C. Smith, and A.B. Flatau, *Structural magnetic strain model for magnetostrictive transducers.* Magnetics, IEEE Transactions on, 2000. **36**(3): p. 545-556.
23. Otsuka, K. and X. Ren, *Recent developments in the research of shape memory alloys.* Intermetallics, 1999. **7**(5): p. 511-528.
24. Dubois, P., et al., *Microactuators based on ion implanted dielectric electroactive polymer (EAP) membranes.* Sensors and Actuators A: Physical, 2006. **130-131**: p. 147-154.
25. Morgan, N.B., *Medical shape memory alloy applications--the market and its products.* Materials Science and Engineering A, 2004. **378**(1-2): p. 16-23.
26. Shen, Y., M.F. Golnaraghi, and G.R. Heppler, *Experimental research and modeling of magnetorheological elastomers.* Journal of Intelligent Material Systems and Structures, 2004. **15**(1): p. 27-35.
27. Bar-Cohen, Y. *Electroactive polymers (EAP) as actuators for potential future planetary mechanisms*. in *Evolvable Hardware, 2004. Proceedings. 2004 NASA/DoD Conference on*. 2004.
28. Zrinyi, M., et al., *Direct observation of abrupt shape transition in ferrogels induced by nonuniform magnetic field.* Journal of Chemical Physics, 1997. **106**(13): p. 5685.
29. Tetsu, M., et al., *Magnetism and compressive modulus of magnetic fluid containing gels.* Journal of Applied Physics, 1999. **85**(12): p. 8451-8455.
30. Hernández, R., et al., *Viscoelastic properties of poly(vinyl alcohol) hydrogels and ferrogels obtained through freezing-thawing cycles.* Polymer, 2004. **45**(16): p. 5543-5549.
31. Ramanujan, R.V. and L.L. Lao, *The mechanical behavior of smart magnet–hydrogel composites.* Smart Materials and Structures, 2006.

15(4): p. 952-956.

32. Liu, T.-Y., et al., *Preparation and characterization of smart magnetic hydrogels and its use for drug release.* Journal of Magnetism and Magnetic Materials, 2006. **304**(1): p. e397-e399.
33. Ryhanen, J., et al., *Biocompatibility of nickel-titanium shape memory metal and its corrosion behavior in human cell cultures.* Journal of Biomedical Materials Research, 1997. **35**(4): p. 451-457.
34. Entel, P., R. Meyer, and K. Kadau, *Molecular dynamics simulations of martensitic transitions.* Philosophical Magazine B-Physics of Condensed Matter Statistical Mechanics Electronic Optical and Magnetic Properties, 2000. **80**(2): p. 183-194.
35. Falcioni, J.G., *Shape Memory Alloys.* Mechanical Engineering, 1992. **114**(4): p. 114-114.
36. Wu, M.H. and L.M. Schetky. *INDUSTRIAL APPLICATIONS FOR SHAPE MEMORY ALLOYS*. in *Shape Memory and Superelastic Technolgies*. 2000. Pacific Grove, California.
37. Newbury, K., *Characterization, Modeling, and Control of Ionic Polymer Transducers*, in *Mechanical Engineering of the Virginia Polytechnic Institute and State University*. 2002, the Virginia Polytechnic Institute and State University: Blacksburg, Virginia.
38. Birmingham, U.o., *Magnetic Materials*, Applied Alloy Chemistry Group.
39. Zrinyi, M., L. Barsi, and A. Buki, *DIRECT OBSERVATION OF DISCRETE AND REVERSIBLE SHAPE TRANSITION IN MAGNETIC FIELD SENSITIVE POLYMER GELS*. 2002, Department of Physical Chemistry, Technical University of Budapest.
40. Faidley, L.E., M.J. Dapino, and A.B. Flatau, *Characterization of a small Terfenol-D transducer in mechanically blocked configuration*, in *Smart Structures and Materials 2001: Smart Structures and Integrated Systems*, L.P. Davis, Editor. 2001. p. 521-532.
41. Staley, M.E. and A.B. Flatau, *Characterization of energy harvesting potential of Terfenol-D and Galfenol*, in *Smart Structures and Materials 2005: Smart Structures and Integrated Systems*, A.B. Flatou, Editor. 2005. p. 630-640.
42. McKnight, G.P., *Magnetostrictive Materials Background*, Active Materials Lab, UCLA.
43. Basantkumar, R.R., et al., *Integration of thin-film Galfenol with MEMS cantilevers for magnetic actuation.* Ieee Transactions on Magnetics, 2006. **42**(10): p. 3102-3104.

44. Faidley, L.E., et al., *Terfenol-D elasto-magnetic properties under varied operating conditions using hysteresis loop analysis*. 1998. p. 856-865.
45. Ellison, J., *INVESTIGATION OF ACTIVE MATERIALS AS DRIVING ELEMENTS IN A HYDRAULIC-HYBRID ACTUATOR*, in *Aerospace Engineering*. 2004, University of Maryland: College Park.
46. Hall, D.L. and A.B. Flatau, *Nonlinearities, Harmonics, and Trends in Dynamic Applications of Terfenol-D.* Smart Structures and Intelligent Systems, Pts 1 and 2, 1993. **1917**: p. 929-939.
47. Petculescu, G., et al., *Magnetic field dependence of galfenol elastic properties.* Journal of Applied Physics, 2005. **97**(10).
48. Faidley, L.E., et al., *Modulus increase with magnetic field in ferromagnetic shape memory Ni-Mn-Ga.* Journal of Intelligent Material Systems and Structures, 2006. **17**(2): p. 123-131.
49. Lane, R. and B. Craig (2003) *MATERIALS THAT SENSE AND RESPOND:AN INTRODUCTION TO SMART MATERIALS*. The AMPTIAC Quarterly **Volume**, 6
50. Mahendran, M. and K. Puspanathan, *Shape memory effect in ferromagnetic Ni-Mn-Ga alloy.* Synthesis and Reactivity in Inorganic Metal-Organic and Nano-Metal Chemistry, 2006. **36**(1): p. 83-88.
51. Faidley, L.E., *CHARACTERIZATION AND MODELING OF FERROMAGNETIC SHAPE MEMORY Ni-Mn-Ga IN A COLLINEAR STRESS-FIELD CONFIGURATION*, in *Mechanical Engineering*. 2006, The Ohio State University: Columbus.
52. Everitt, B.A., *The design of magnetoresistive devices.* Proceedings of the 39th Midwest Symposium on Circuits and Systems, Vols I-Iii, 1996: p. 119-122.
53. Bogue, R.W., *A Novel Industrial Application for Magnetoresistive Sensors.* Journal of Physics E-Scientific Instruments, 1985. **18**(2): p. 174-178.
54. Gschneidner, K.A., V.K. Pecharsky, and A.O. Tsokol, *Recent developments in magnetocaloric materials.* Reports on Progress in Physics, 2005. **68**(6): p. 1479-1539.
55. Li, W.H., et al., *Nonlinear rheological behavior of magnetorheological fluids: step-strain experiments.* Smart Materials & Structures, 2002. **11**(2): p. 209-217.
56. Kallio, M. (2005) *The elastic and damping properties of magnetorheological elastomers*. VTT PUBLICATIONS **Volume**, 149
57. Ginder, J.M., et al., *Controllable-stiffness components based on magnetorheological elastomers.* Smart Structures and Material 2000: Smart

Structures and Integrated Systems, 2000. **3985**: p. 418-425.

58. Ginder, J.M., et al., *Magnetorheological elastomers: Properties and applications.* Smart Structures and Materials 1999: Smart Materials Technologies, 1999. **3675**: p. 131-138.
59. York, D., X. Wang, and F. Gordaninejad, *A new MR fluid-elastomer vibration isolator.* Journal of Intelligent Material Systems and Structures, 2007. **18**: p. 1221-1225.
60. Klingenberg, D.J., *Magnetorheology: Applications and challenges.* Aiche Journal, 2001. **47**(2): p. 246-249.
61. Neuringe.Jl and Rosenswe.Re, *Ferrohydrodynamics.* Physics of Fluids, 1964. **7**(12): p. 1927-&.
62. Jarkova, E., et al., *Hydrodynamics of isotropic ferrogels.* Physical Review E, 2003. **68**(4).
63. Mitsumata, T., et al., *Magnetism and compressive modulus of magnetic fluid containing gels.* Journal of Applied Physics, 1999. **85**(12): p. 8451-8455.
64. Raikher, Y.L. and V.V. Rusakov, *Viscoelastic ferrogel: Dynamic magnetic susceptibilities.* Brazilian Journal of Physics, 2001. **31**(3): p. 366-379.
65. Chatterjee, J., Y. Haik, and C.J. Chen, *Biodegradable magnetic gel: synthesis and characterization.* Colloid and Polymer Science, 2003. **281**(9): p. 892-896.
66. Collin, D., et al., *Frozen-in magnetic order in uniaxial magnetic gels: Preparation and physical properties.* Macromolecular Rapid Communications, 2003. **24**(12): p. 737-741.
67. Galicia, J.A., et al., *Designing magnetic composite materials using aqueous magnetic fluids.* Journal of Physics: Condensed Matter, 2003. **15**(15): p. S1379-S1402.
68. S.K.Saxena (2004) *POLYVINYL ALCOHOL (PVA)*. 61st JECFA **Volume**, 3
69. Wang, H.H., T.W. Shyr, and M.S. Hu, *The elastic property of polyvinyl alcohol gel with boric acid as a crosslinking agent.* Journal of Applied Polymer Science, 1999. **74**(13): p. 3046-3052.
70. Hassan, C.M. and N.A. Peppas, *Structure and applications of poly(vinyl alcohol) hydrogels produced by conventional crosslinking or by freezing/thawing methods.* Biopolymers/Pva Hydrogels/Anionic Polymerisation Nanocomposites, 2000. **153**: p. 37-65.
71. Chu, K.C. and B.K. Rutt, *Polyvinyl alcohol cryogel: An ideal phantom material for MR studies of arterial flow and elasticity.* Magnetic Resonance in Medicine, 1997. **37**(2): p. 314-319.
72. Mori, Y., H. Tokura, and M. Yoshikawa, *Properties of hydrogels synthesized*

by freezing and thawing aqueous polyvinyl alcohol solutions and their applications. Journal of Materials Science, 1997. **32**(2): p. 491-496.

73. Jonathan Thomas, K.G.A.L.M.M., *The effect of dehydration history on PVA/PVP hydrogels for nucleus pulposus replacement.* Journal of Biomedical Materials Research Part B: Applied Biomaterials, 2004. **69B**(2): p. 135-140.
74. Barsi, L. and M. Zrinyi, *Ferrogels as magnetomechanical actuators.* ACH-Models in Chemistry, 1998. **135**: p. 241-246.
75. tnsft.com. *Summary of Concepts in Performance and Reliability Diagnosis*. 2007 [cited 2008 April 30].